SUPPLEMENTAL MATERIAL

Methods

Generation of Calm1$^{N98S/+}$ mice. We used the CRISPR/Cas9 gene editing approach to generate knock in mice heterozygous for the N98S mutation in the *Calm1* gene.[22] Zygotes isolated from C3HeB/FeJ mice were injected with a mixture containing guide RNA targeting exon 5 of the *Calm1* gene, capped mRNA encoding Cas9, and a 193-nucleotide single-stranded donor oligonucleotide with DNA spanning the target site and carrying an AT to GC nucleotide substitution. This nucleotide change results in an asparagine (AAT) to serine (AGC) amino acid substitution at Calm1 amino acid residue 98, and concomitantly introduces a *BsrB1* restriction site (CCGCTC; Supplemental Figure I A). The injected embryos were transferred to pseudopregnant Swiss Webster females. Offspring was screened for the N98S Calm1 mutation by using a PCR-based restriction fragment length polymorphism (RFLP) assay (Supplemental Figure I B and C).[22] Genomic DNA from mice was extracted and used in PCRs with *Calm1* gene-specific primers (PCR primer sequences are listed at the end of the Supplemental Data) under the following conditions: 95° for 4 min; 35x (95° for 1 min, 66° for 2 min, 72° for 3 min); 72° for 7 min, hold at 4 °. A total of 5 μl of *Calm1* PCR products were digested with *BsrB1* and separated on acrylamide gel (8 %) for detection of CRISPR/Cas9-mediated mutation. PCR products were cloned into the Topo vector (Thermo Fisher Scientific, Waltham, MA), and sequences of individual clones were determined by Sanger sequencing. Among 30 mice derived from zygote injections, we identified two male founder mice carrying the mutant allele. Sequence analysis of cloned PCR products confirmed that both mice acquired the N98S substitution (not shown). These animals were then crossed into a C57BL/6J genetic background to establish two independent mouse lines, designated line 2 and line 18. Mice heterozygous for the N98S *Calm1* mutation (Calm1$^{N98S/+}$) are viable and survive to adulthood. No sudden deaths were observed in mice of either genotype from either line. The expected Mendelian ratios

(observed/expected genotypes) for Calm1$^{+/+}$ mice at weaning ages were 117/218 and 71/146 for line 2 (P = 0.74 by χ^2) and line 18 (P = 0.91 by χ^2), respectively. Adult (i.e., > 3 months of age) mice from F4 to F6 backcross generations were used for experiments. No differences in the body weight between Calm1$^{+/+}$ and Calm1$^{N98S/+}$ mice of either line were observed (line 2: 33.5 ± 1.5 g, Calm1$^{+/+}$, N = 11; 31.8 ± 1.4 g, Calm1$^{N98S/+}$, N = 8; line 18: 36 ± 1.8 g, Calm1$^{+/+}$, N = 7; 40.6 ± 2.2 g, Calm1$^{N98S/+}$, N = 7). Four-chamber sections of adult Calm1$^{N98S/+}$ hearts did not reveal any alterations (Supplemental Figure II). Examples displayed in Supplemental Figure II are representative of 3 hearts examined per line and genotype. Transthoracic echocardiography in anesthetized adult mice (line 2) revealed no significant differences between the genotypes for wall thickness, chamber dimensions, or contractile indices (Supplemental Figure II B and Supplemental Table I).

Telemetry. ECG telemetry devices (F10, Data Science International, St. Paul, MN, USA) were implanted intra-abdominally under isoflurane anesthesia and connected to two wire electrodes placed subcutaneously in a lead-II configuration. Recordings were initiated 2-3 days after recovery from surgery. Mice carrying telemetry devices were exposed to 12-hour light/dark cycles (light, 6:00 AM to 6:00 PM; dark, 6 PM to 6 AM). After an initial 24-hour recording period, telemetered mice routinely received intraperitoneal injections of caffeine (120 mg per kg body weight) and epinephrine (2 mg per kg body weight) to assess their susceptibility to inducible arrhythmia. Mean RR intervals were calculated from 5- to 10-s samples evaluated at 20-min steps throughout the 24-h recording period. Signal-averaged ECGs were obtained from the same samples, by overlaying all the cycles within each sample using the QRS maximum or minimum as fiduciary points, and PR, QRS and QT intervals were measured as outlined above. The heart-rate corrected QT interval (QT_c) was calculated by using the following equation:

$$QT_c = \frac{QT}{\left(RR/110\right)^n}, \quad (1)$$

where *RR* and *QT* represent the mean RR and mean QT interval, respectively, within each 5- to 10-s sample of a 24-h ECG recording. The RR intervals are expressed as unitless multiples of 110 ms, which corresponds to the mean of the average 24-h RR intervals in conscious Calm1$^{+/+}$ and Calm1$^{N98S/+}$ mice. The value of the exponent, *n*, was evaluated by assessing the slope of the relationship between the natural logarithms of each of these variables, i.e., ln (QT) = ln (QT_c) + *n* ln (RR/110), using linear regression analysis (an example is shown in Supplemental Figure III).[37]

Calculation of ventricular arrhythmia score. Arrhythmia score was defined by the worst ventricular arrhythmia (1 – no or isolated premature ventricular contractions (PVCs), 2 – ventricular bigeminy and/or frequent PVCs (>10/min), 3 – ventricular couplet, 4 – nonsustained ventricular tachycardia (lasting ≥ 4 s and ≤ 15 s).[38]

Treadmill exercise. After a 72-hour recovery period following implantation of the telemetry device, telemetered ECGs were recorded continuously for 24 hours. Mice were then exercised on a single-lane graded treadmill (model LE8708, Harvard Apparatus, Cambridge, MA). Mice initially ran at a speed of 10 m/min and slope of 15 degrees, and speed was increased by 2 m/min very minute until they reached exhaustion. Exhaustion was defined as the mouse spending more than 50% of the time or more than 15 seconds consecutively on the shock grid.[14]

Epicardial optical voltage mapping of Langendorff-perfused hearts. High-resolution optical mapping experiments were performed on 4- to 6-month old Calm1$^{N98S/+}$ and littermate Calm1$^{+/+}$ mice as described previously.[39] Hearts were isolated and retrogradely perfused in Langendorff-mode with temperature-controlled (37°C) Krebs-Henseleit solution (pH 7.4 when gassed with a mixture of 95% O_2 and 5% CO_2) at an aortic pressure of 70 cm H_2O. A volume-conducted ECG was monitored continuously throughout the experiment. After 10 minutes of stabilization, the hearts were stained with the voltage-sensitive dye Di-4-ANEPPS (2 µL of a 2-mmol/L stock

solution). The heart was then washed with dye-free solution for 5 min followed by the addition of (±)-blebbistatin to uncouple contraction from excitation (10 μmol/L; Tocris Bioscience, Minneapolis, MN). The stained hearts were illuminated with a laser at a 532 nm wavelength and the fluorescence was collected by a MiCAMUltima-L CMOS camera (SciMedia, Costa Mesa, CA) through a 715-nm long-pass filter. The fluorescence was recorded at a 1 ms/frame rate in a 100×100 pixel grid with a spatial resolution of 0.35×0.35 mm^2 per pixel. Optical signals were processed with both spatial (3×3 pixels Gaussian filter) and temporal (3 frames moving average) filtering. Hearts were paced at the right atrium at a cycle length of 120 ms throughout the duration of the experiment. Four 1-s recordings were captured in 5-min intervals starting 20 min after begin of (±)-blebbistatin perfusion. Signals were averaged across the entire map and these spatially averaged signals were used to measure APD at 30, 50 and 80% repolarization (APD_{30}, APD_{50} and APD_{80}). Because values for APD were not significantly different among the four time points ($P > 0.05$ by *Repeated Measures ANOVA*), they were lumped together into a single value. Conduction velocity was measured as described previously.[39] After the fourth recording, hearts were perfused with a solution containing epinephrine (1.6 μmol/L) and caffeine (5 mmol/L) and/or heightened external [Ca^{2+}] (3.6 mmol/L) plus isoproterenol (100 or 200 nmol/L) to assess arrhythmia susceptibility. In a subset of hearts, programmed electrical stimulation and ventricular burst stimulation in the presence of isoproterenol (100 nmol/L) and elevated external [Ca^{2+}] (3.6 mmol/L) were also used to assess inducibility of ventricular arrhythmias. Rectangular, 2-ms stimuli were delivered to the apex at twice the pacing threshold current. Ventricular refractory period was obtained by S1S2 stimulation with trains of 8 S1 stimuli (100, 90 and 80 ms) and decremental coupling of S2 intervals (2-ms decrement). To induce arrhythmias, two protocols were used:

1) Programmed electrical stimulation: two (S2S3) and three (S2S3S4) extrastimuli (initial coupling interval 60 ms, 2-ms decrement) after a train of eight S1 stimuli (cycle lengths

100, 90 and 80 ms). When coupling 2 extrastimuli, the first extrastimulus was delivered at 20 ms above the refractory period and the second extrastimulus was coupled at an interval from 60 ms to refractoriness in 2-ms decrements. When coupling 3 extrastimuli, the first and second extrastimuli were delivered at 20 ms above the refractory periods and the third extrastimulus was coupled at an interval from 60 ms to refractoriness in 2-ms decrements.

2) Burst stimulation: 1-s trains of 2-ms stimuli at frequencies of 20, 25, 33, 50 and 100 Hz.

Interval between each train or burst was 5 s.

Histology. Hearts were immersion fixed with Flowfix for ~12 hours at 4 °C, cryoprotected with 30% sucrose in PBS for ~12 hours, and embedded in OCT (Fisher Scientific, Waltham, MA) Ten-μm longitudinal sections were cut on a cryotome (CM1860, Leica, Wetzlar, Germany). The sections were stained with Hematoxylin & Eosin (Sigma-Aldrich, St. Louis, MO) and examined under a light microscope. Images were captured with a digital camera (DS126311, Canon, Japan) using a 4x objective.

Quantitative rt-PCR. RNA was extracted from mouse heart tissue using TRIzol Reagent (Thermo Fisher Scientific 15596026). Reverse transcription was performed by PrimeScript™ RT reagent Kit (Clontech, RR037A). Real-time PCR reactions were performed using Power SYBR Green PCR Master Mix (Thermo Fisher Scientific, 4367659) with an Applied Biosystems realplex, and the primer sets were tested to be quantitative. Transcription factor IIb (TFIIb) was used as normalizer. Threshold cycles and melting curve measurements were performed with ABI software. *P*-values were calculated by the Student-*t* test. Error bars indicate standard error of mean.

Transmembrane action potential recordings from the right ventricular conduction system

We used standard microelectrode techniques to record transmembrane action potentials from cells of the right ventricular conduction system, including the right bundle branch and free running strands. Experiments were carried out in the septal wedge preparation as previously described by Anumonwo et al.[40] Hearts were excised, the atria as well as the right and left ventricular free walls were removed, and the remaining wedge of septal tissue was pinned down in a perfusion chamber with the right side facing up and continuously superfused with oxygenated normal Tyrode's solution. Measurements were performed using the standard microelectrode technique (DC resistance of ~20 MΩ when filled with 3 M KCl) at 37 ± 1℃ while the preparation was being viewed under a dissecting microscope. The preparations were driven using a bipolar stimulation electrode at pulse amplitudes of ~0.2 mA, pulse duration of 2 ms, and a basic cycle length of 200 ms. The pacing electrode was placed at the base of the wedge. Pacing was interrupted twice for 10 s each to examine whether afterdepolarizations could be induced. The same protocol was repeated after the addition of 100 nM isoproterenol and after 5 min washout. All data acquisition and analyses were carried out using Axoscope and pClamp software, respectively (Molecular Devices).

Action potentials from the right bundle branch and the web exhibited spontaneous diastolic depolarizations and/or morphologies that were distinctly different from those of endocardial septal myocytes but identical to those previously reported for isolated cardiomyocytes expressing a conduction-system specific fluorescent reporter (Supplemental Figure XIV A),[41] indicating the suitability of the wedge preparation to capture the distinct electrical characteristics of ventricular conduction fibers.

Cellular Electrophysiology

Isolation of single ventricular myocytes. Mouse left ventricular myocytes were isolated enzymatically by a protocol described previously.[39] Following inhalation anesthesia with 5% isoflurane / 95% O_2 the mice were euthanized by cervical dislocation and the hearts were removed immediately via thoracotomy. After retrograde perfusion with nominally Ca^{2+}-free, oxygenated Tyrode's solution for 5 min, the heart was perfused with the same solution containing 200 U/ml collagenase (Worthington type II; Worthington Biochemical Corporation, Lakewood, NJ) for ~10 min. Next, the heart was transferred to a dish filled with 0.1 mmol $CaCl_2$Tyrode's solution, the right ventricular free wall and the atria were removed, the left ventricular free wall was minced into small pieces, triturated and filtered through a 100-µm Nylon mesh. The filtered cells were centrifuged at 500 rpm for 1 min. The supernatant was removed, and the cell pellet was resuspended in 0.2 mmol/L $CaCl_2$ Tyrode's solution. Centrifugation was repeated, the resuspended cells were stored in 0.5 mmol/L $CaCl_2$ Tyrode's solution and used within 6-8 h. Only calcium tolerant, quiescent, and rod-shaped cells were studied.

Transmembrane action potential recordings. Action potentials were recorded at 36 – 37 °C in the fast current-clamp mode of an Axopatch 200B amplifier (Molecular Devices, Sunnyvale, CA). Microelectrodes were pulled from borosilicate glass capillaries (Sutter Instruments, Novato, CA) using a Sutter P-97 puller (Sutter Instruments) and had a tip resistance of 1.8 to 2.5 MΩ when filled with pipette solution. Action potentials were evoked by a 2-ms injection of depolarizing current (1.0 – 1.2 nA) at a frequency of 1 Hz. Signals were filtered at 10 kHz and sampled at 25 kHz. The following action potential parameters were measured: resting membrane potential, phase 0 action potential amplitude, maximal phase 0 upstroke velocity (dV/dt_{max}), and action potential duration (APD) at 30, 50 and 90% repolarization (APD_{30}, APD_{50} and APD_{90}). Delayed afterdepolarizations were defined as spontaneous diastolic depolarizations of ≥ 5 mV and lasting at least 10 ms.

Whole-cell $I_{Ca.L}$ *recordings.* Voltage-clamp recordings were performed at room temperature in standard whole-cell configuration. Microelectrodes were pulled from borosilicate glass capillaries (Sutter Instruments) using a Sutter P-97 puller and had a tip resistance of 1.8 to 2.5 MΩ when filled with pipette solution. Currents were acquired using an Axoptach 200B and Clampex10 software (Molecular Devices), low-pass filtered at 1 kHz, and sampled at 5 kHz. The pipette potential was zeroed before seal formation, and voltages were not corrected for liquid junction potential. Leakage currents were digitally subtracted online using a P/4 protocol of Clampex10. Capacitance transients were cancelled using the computer-controlled circuitry of the amplifier, and voltage errors were minimized using 60-70% series resistance compensation. Series resistance before compensation was typically 5-9 MΩ. After establishing the whole-cell configuration, the myocytes were allowed to equilibrate for 10 min with the internal solute before the data were collected.

To characterize voltage dependence of peak $I_{Ca.L}$ and to determine the $I_{Ca.L}$ activation curves, currents were evoked by 300-ms pulses ranging from -50 to +60 mV in steps of 10 mV. The interval between voltage steps was 5 s. The peak $I_{Ca.L}$ density at each potential was plotted as a function of test voltage to generate the *I-V* curves. Activation curves were fitted with the following Boltzmann distribution equation: $G/G_{max} = 1/\{1+\exp[V_{1/2} - V)/k]\}$, where G is the voltage-dependent calcium conductance, G_{max} is the maximal calcium conductance, $V_{1/2}$ is the potential at which activation is half-maximal, V is the membrane potential, and k is the slope. G values were determined by the following equation: $G = I_{max}/(V-E_{Ca})$, where E_{Ca} is the reversal potential.

To examine steady-state inactivation, the voltage that gave maximal peak current was used for subsequent protocols. Cells were administered a series of prepulses (-70 to 50 mV) lasting 300 ms, from the holding potential of -70 mV, followed by a 300-ms depolarization to a voltage eliciting the maximal peak current (10 mV), every 10 s. The resulting curves were

normalized and fitted using the following Boltzmann distribution equation: $I/I_{max} = 1/\{1 + \exp[(V - V_{1/2})/k]\} + C$, where I_{max} is the peak current elicited after the most hyperpolarized prepulse, V is the preconditioning pulse potential, and C is a constant.

To examine the time course of $I_{Ca.L}$ recovery from inactivation, cells were held at -70 mV and were administered a 300-ms conditioning pulse to 10 mV, followed by a variable time period at -70 mV and a test pulse of 300 ms to 10 mV. Interval between prepulses was 10 s. Recovery from inactivation was quantitated by fitting data for each cell using the following Equation:

$I_{test}/I_{cond} = [1 - \exp(-t/\tau)]$,

where t is time, τ is the time constant, and I_{cond} is the peak $I_{Ca.L}$ during the preconditioning pulse.

To quantify the kinetics of $I_{Ca.L}$ inactivation, the decay phase of $I_{Ca.L}$ was fitted using a mono-exponential function of the form: $I(t) = A * \exp(-t/\tau) + A_{ss}$, where t is time, τ is the time constant of decay of the inactivating $I_{Ca.L}$, A is the amplitude of the inactivating current component, and A_{ss} is the non-inactivating component of the total $I_{Ca.L}$. Time zero was set at the peak of the inward current.

The membrane capacitance was calculated from 5-mV hyperpolarizing and depolarizing steps (20 ms) applied from a folding potential of -70 mV according to the equation:

$C_M = \tau/\Delta V * I_0/(1 - I_\infty/I_0)$,

where C_M is membrane capacitance, τ is the time constant of the capacitance current relaxation, I_0 is the peak capacitive current determined by single exponential fit and extrapolation to the first sample point after the voltage step ΔV, and I_∞ is the amplitude of the steady-state current during the voltage step.[42] Capacitive currents were sampled at 25 kHz and filtered at 5 kHz.

Whole-cell I_{Na} recordings. To characterize voltage-dependence to peak I_{Na} and to determine the I_{Na} activation curves, currents were evoked by 40-ms square pulses ranging from -80 to +60 mV in steps of 5 mV. Holding potential was -120 mV. The interval between voltage steps was 3 s.

I_{Na} activation curves were generated and fitted as outlined above for $I_{Ca.L}$. For steady-state inactivation measurements, cells were administered a series of prepulses (-120 to -10 mV) lasting 500 ms, from a holding potential of -120 mV, followed by a 20-ms depolarization to -10 mV, every 3 s. The resulting curves were analyzed as described for $I_{Ca.L}$ above. To investigate the time course of I_{Na} recovery from inactivation, cells were held at -120 mV and were administered a 1000-ms conditioning pulse to -10 mV, followed by a variable time period at -120 mV and a 10-ms test pulse to -10 mV. Interval between prepulses was 3 s. To quantify the kinetics of I_{Na} inactivation, the decay phases of I_{Na} was fitted using a double-exponential function: $y(t) = A_{fast}\exp(-t/\tau_{fast}) + A_{slow}\exp(-t/\tau_{slow}) + y_{0.}$

For measurements of late I_{Na}, currents were elicited at -30 mV (for 1,000 ms) from a holding potential of -120 mV and leak corrected using a P/4 protocol. Current was integrated between 30 and 530 ms.

Analyses of electrophysiological recordings was performed using the Clampfit module of pClamp10 (Molecular Devices).

Confocal Ca^{2+} imaging. $[Ca^{2+}]_i$ transients and sparks were recorded in intact ventricular myocytes loaded with fluorescent Ca^{2+} dye Fluo-4 AM, on a laser scanning confocal microscope (Leica) equipped with a 40x oil immersion lens (NA = 1.3). Fluo-4 (loaded by 20 min incubation with 10 μM of acetoxymethylester dissolved in normal Tyrode's solution supplemented with F-127. Fluo-4 was excited with the 488-nm line of an argon laser. Fluorescence was collected through a 515- to 560-nm bandpass filter. Fluo-4 images were recorded in line-scan mode with 512 pixels per line at 600 Hz. To record cell-wide $[Ca^{2+}]_i$ transients, cells were excited at 0.5, 1, 2 or 3 Hz by field stimulation using two parallel platinum electrodes. Spontaneous Ca^{2+} sparks were acquired in quiescent cells after steady state stimulation at a rate of 1 Hz.

Ca^{2+} sparks were analyzed using Spark Master.[43] We used spark detection threshold 3.8 x s.d.. Ca^{2+} spark amplitudes were normalized ($\Delta F/F_o$) to fluorescence baseline (F_o). Duration of Ca^{2+} sparks was taken as the duration at 50% of peak (full duration at half maximum, FDHM). Width of Ca^{2+} sparks was the spatial size at 50% of peak (full width at half maximum, FWHM).

To determine the properties of action potential-evoked changes in fluo-4 fluorescence, we first calculated the average signal intensity of each successive line in a line-scan image, to obtain the time course of the line average fluorescence, *F(t)*. The F(t) traces were condensed into one-cycle recordings by averaging over three consecutive transients, and converted to -$\Delta F/F_0(t)$, where F_0 is the average *F* over the time before the Ca^{2+} rise, and ΔF equals $F_{(t)}$-F_0. From the averaged $\Delta F/F_0(t)$ we determined the magnitudes of peak $\Delta F/F_0$, and 30%, 50% and 80% recovery.

Solutions. The Tyrode's solution for cell isolation contained (in mM) 133.5 NaCl, 4 KCl, 0.1, 0.2 or 0.5 $CaCl_2$, 1.2 $MgSO_4$, 1.2 NaH_2PO_4, 10 HEPES, 11 D-glucose, pH 7.4, with NaOH.

Bath solution for $I_{Ca.L}$ recording contained (in mM) 140 TEA-$MeSO_3$, 10 HEPES (pH 7.4); and 5 $CaCl_2$ or $BaCl_2$ (or 1.8 $CaCl_2$) at 300 mOsm, adjusted with TEA-$MeSO_3$. Pipette solution 1 for $I_{Ca.L}$ recording contained (in mM): 114 $CsMeSO_3$; 5 CsCl; 1 $MgCl_2$; 4 MgATP; 10 HEPES (pH 7.3); 10 BAPTA; and 0.005 ryanodine; at 295 mOsm adjusted with $CsMeSO_3$. Pipette solution 2 for $I_{Ca.L}$ recording contained (in mM): 114 $CsMeSO_3$; 5 CsCl; 1 $MgCl_2$; 4 MgATP; 10 HEPES (pH 7.3); 1 EGTA; at 295 mOsm adjusted with $CsMeSO_3$.

Bath solution for I_{Na} recording contained (in mM) 5 NaCl, 15 TEACl, 110 CsCl, 1.2 $MgCl_2$, 1.5 $CaCl_2$, 10 HEPES, 5 glucose, 5 sucrose, 5 $CoCl_2$ (pH 7.4 adjusted with CsOH). The pipette solution for I_{Na} recording contained (in mM) 124 L-aspartic acid, 2.5 Na_2ATP, 10 HEPES, 11 EGTA, 1 $CaCl_2$, 2 $MgCl_2$ (pH 7.3 adjusted with CsOH). For late I_{Na} recordings, pipettes were filled with (in mM) 40 CsCl, 80 Cs-glutamate, 10 NaCl, 0.92 $MgCl_2$, 5 Mg-ATP, 0.3 Li-GTP, 10

HEPES, 0.03 niflumic acid, 0.02 nifedipine, 0.004 strophanthidin, 5 BAPTA (tetracesium salt), 1 5,5′-dibromo BAPTA (tetrapotassium salt), and 3.73 mM $CaCl_2$ (free $[Ca^{2+}]_i$, 500 nM) (pH 7.2 adjusted with CsOH). The bath solution contained (in mM) 10 NaCl, 130 tetramethylammonium chloride, 4 CsCl, 1 $MgCl_2$, 10 glucose, 10 HEPES, and 0.0001 thapsigargin (pH 7.4 adjusted with NaOH).

For action potential recording from single myocytes, the bath solution contained (in mmol/L): 135 NaCl; 5.4 KCl; 1.8 $CaCl_2$; 0.33 $MgCl_2$; 0.33 NaH_2PO_4; 5 HEPES; and 5 glucose (pH 7.4). Pipette solution contained (in mM): 130 K glutamate; 9 KCI; 10 NaCl; 0.5 $MgCl_2$; 0.5 EGTA; 4 MgATP; and 10 HEPES (pH 7.3 with KOH). Osmolarities of bath and pipette solutions were adjusted to 310 mosm/L.

For microelectrode recordings from septal wedges, the bath solution contained (in mmol/L) 1335. NaCl, 4 KCl, 1.8 $CaCl_2$, 1.2 $MgSO_4$, 1.2 NaH_2PO_4, 10 HEPES, 11 glucose (pH 7.4, adjusted with NaOH).

Line 2 was used in optical mapping experiments and in His-Purkinje myocyte action potential recordings as well in all single-cell experiments, including measurements of $[Ca^{2+}]_i$, transmembrane voltage, whole-cell $I_{Ca.L}$ and I_{Na}.

Primer sequences for PCR

Forward: GGGGGAGGGTTGGGGTACAGAGTTGGCATT
Reverse: CTGAAGACTACACTTAGCCTTTACCTTCAT

Sequence of donor oligonucleotide

ATTCAGAGAGATTGTCCTCTTAAAACCGCCATCCCCCAGTGCCTTGTAACGTCATTGCTTGTTCACAGGATGG
GAGCGGTTACATCAGCGCCGCAGAGCTGCGGCACGTCATGACAAACTTAGGAGAAAAGCTAACAGATGAAG
AAGTAGATGAAATGATCAGAGAAGCAGATATTGATGGCGA

Sequence of the 193-bp donor oligonucleotide for CRISPR/Cas9-mediated generation of N98S *Calm1* knock in mice. Oligonucleotide-directed 2-bp change is highlighted in yellow. The *BsrB1* recognition site is underlined.

sgRNA target sequence

CCACGTCATGACAAACTTAGGAG (antisense)

The protospace adjacent motif is highlighted in green.

Primer sequences for rt-PCR of *Calm1*, *Calm2* and *Calm3*

Calm1 F: TGTCCGTGGTGCCGTTACTC;

Calm1 R: CTGATCAGCCATGGTGCGAG.

Calm2 F；GTGGAGCGAGCGAGTCGAG；

Calm2 R: TTTGAACTCTGCAATCTGCTCTTC.

Calm3 F: AGTAACCTCGATCCCCGAGC;

Calm3 R: TGGTGCCATCTCCATCCTTG.

TFIIb F: CTCTGTGGCGGCAGCAGCTATTT

TFIIb R: CGAGGGTAGATCAGTCTGTAGGA

Results

Absence of exercise-induced sustained ventricular arrhythmias in Calm1N98S/+ mice

To evoke arrhythmias, we subjected mice to treadmill exercise followed by epinephrine injection (2 mg per kg body weight i.p.) while continuously monitoring their ECG by telemetry. Maximal running time on the treadmill was not significantly different between $Calm1^{+/+}$ mice (20.7 ± 0.9 min; n = 5) and $Calm1^{N98S/+}$ mice (21.1 ± 2.2 min, n = 4; P = 0.88 by t-test). The average incidence of premature ventricular contractions during a 30-min post-exercise recording period was similar in the two groups of mice ($Calm1^{+/+}$: 1.7 ± 1.2 , $Calm1^{N98S/+}$: 3 ± 1.2 ; $P > 0.05$ by χ^2). Episodes of sustained VT were not observed.

Properties of cardiac L-type Ca^{2+} current under conditions of high intracellular Ca^{2+} buffering

Supplemental Figure VIII A shows exemplar families of macroscopic L-type Ca^{2+} current traces elicited by 300-ms steps to voltages between -50 and 100 mV from a holding potential of -50 mV, revealing rapidly activating and slowly inactivating currents in both cells. Mean peak $I_{Ca.L}$ density-voltage relationships from $Calm1^{+/+}$ and $Calm1^{N98S/+}$ myocytes were superimposable (Supplemental Figure VIII B) as were the curves for voltage-dependence of steady-state activation and inactivation (Supplemental Figure VIII C; fit parameters in Supplemental Table V). Supplemental Figure VIII D displays representative Ca^{2+} currents evoked by step depolarizations to +10 mV in a $Calm1^{+/+}$ and $Calm1^{N98S/+}$ myocyte, demonstrating slower current decay in the latter. On average, the time constant for whole-cell $I_{Ca.L}$ decay was significantly larger in $Calm1^{N98S/+}$ myocytes (Supplemental Figure VIII E), indicating that N98S-CaM attenuates L-type channel inactivation, in agreement with previously published observations.[10] Replacement of external Ca^{2+} with equimolar Ba^{2+} which binds only poorly to CaM, abrogated differences in decay kinetics (Supplemental Figure VIII F). On average, the fraction of peak current remaining after 300-ms depolarization to +10 mV (r_{300}) was higher in $Calm1^{N98S/+}$ myocytes when Ca^{2+}, but not Ba^{2+}, was the charge carrier, indicating that N98S CaM blunts CDI (Supplemental Figure VIII F). To quantify the extent of CDI, the differences between Ba^{2+} and Ca^{2+} r_{300} relations were normalized to the corresponding Ba^{2+} r_{300} values [$f_{300} = (r_{300/Ba} - r_{300/Ca})/r_{300/Ba}$], revealing a significantly smaller mean f_{300} in $Calm1^{N98S/+}$ versus $Calm1^{+/+}$ myocytes, consistent with N98S-CaM-mediated impairment of CDI (Supplemental Figure VIII G). As one would expect from attenuated L-type channel inactivation, $I_{Ca.L}$ recovery from inactivation was faster in $Calm1^{N98S/+}$ myocytes (Supplemental Figure VIII I), as evidenced by a shorter time constant of recovery (Supplemental Figure VIII J and Supplemental Table V). Taken together, these results suggest that CDI of L-type channels is attenuated in $Calm1^{N98S/+}$ ventricular myocytes. The magnitude of f_{300} in $Calm1^{N98S/+}$ myocytes is in close agreement with that previously measured in HEK293 cells co-transfected with *CACNA1C* ($Ca_v1.2$) and N98S *CALM1*.[10]

Supplemental Tables

Supplemental Table I. Echocardiographic Data

	Calm1$^{+/+}$ **N = 7**	**Calm1$^{N98S/+}$** **N = 8**
Heart Rate, min^{-1}	504 ± 22	400 ± 22 *
IVSd, mm	0.92 ± 0.06	0.97 ± 0.04
IVSs, mm	1.42 ± 0.07	1.40 ± 0.05
LVIDd, mm	3.54 ± 0.12	3.47 ± 0.17
LVIDs, mm	2.09 ± 0.08	2.00 ± 0.10
LVPWd, mm	0.97 ± 0.06	0.95 ± 0.05
LVPWs, mm	1.38 ± 0.06	1.38 ± 0.08
EDV, μL	53.0 ± 4.2	51.2 ± 5.8
ESV, μL	14.4 ± 1.4	13.1 ± 1.5
EF, %	78.7 ± 0.5	79.5 ± 0.9
FS, %	41.2 ± 0.4	42.1 ± 0.9

Values are mean ± SEM. IVSd and IVSs, interventricular septum diastolic and systolic; LVIDd and LVIDs, left ventricular internal diameter, diastolic and systolic; LVPWd and LVPWs, left ventricular posterior wall, diastolic and systolic; EDV, end-diastolic volume; ESV, end-systolic volume; EF, ejection fraction; FS, fractional shortening. * $P = 0.0022$ versus Calm1$^{+/+}$ by *t*-test.

Supplemental Table II. mRNA in Calm1$^{+/+}$ and Calm1$^{N98S/+}$ littermates

Genotype	*Calm1*	*Calm2*	*Calm3*
Calm1$^{+/+}$ N = 7	1.01 ± 0.06	1.02 ± 0.09	1.02 ± 0.10
Calm1$^{N98S/+}$ N = 7	1.23 ± 0.17	1.27 ± 0.09	1.23 ± 0.15

Values are mean ± SEM expressed relative to Calm1$^{+/+}$.

Supplemental Table III. Frequency dependence of ventricular action potential properties

	Calm1$^{+/+}$		**Calm1$^{N98S/+}$**	
	n = 11; N = 3		n = 11; N = 4	
	1 Hz	**7 Hz**	**1 Hz**	**7 Hz**
RMP, mV	-69.0 ± 1.2	-68.0 ± 1.2	-70.3 ± 1.1	-69.7 ± 1.4
APA, mV	123.6 ± 1.3	118.3 ± 2.0 *	123.4 ± 2.3	119.8 ± 2.6
dV/dt_{max}, V/s	269 ± 25	222 ± 21 **	250 ± 22	229 ± 23
APD_{30}, ms	2.6 ± 0.5	3.0 ± 0.6	2.2 ± 0.3	2.4 ± 0.4
APD_{50}, ms	6.3 ± 1.1	7.2 ± 1.5	6.3 ± 1.2	6.7 ± 1.0
APD_{90}, ms	43.5 ± 5.4	47.4 ± 8.6	37.1 ± 4.6	47.7 ± 6.6 #

Values are mean ± SEM. N and n indicate number of mice and cells, respectively. RMP, resting membrane potential; APA, action potential amplitude; $dVdt_{max}$; maximal phase 0 upstroke velocity; APD, action potential duration. * P = 0.016 vs. 1 Hz; ** P = 0.04 vs. 1 Hz; # P = 0.004 vs. 1 Hz. P values by paired t-tests. No significant differences were found for any parameter between the two genotypes (t-test).

Supplemental Table IV. Effect of isoproterenol on ventricular myocyte action potentials.

	Calm1$^{+/+}$			**Calm1$^{N98S/+}$**		
	n = 14; N = 5			n = 10; N = 4		
	Control	**Iso**	**WO**	**Control**	**Iso**	**WO**
RMP, mV	-68.5 ± 0.9	-69.0 ± 0.9	-68.5 ± 1.0	-67.4 ± 0.6	-67.0 ± 0.7	-66.4 * ± 0.7
APA, mV	124.5 ± 1.3	124.2 ± 1.0	123.3$^{\|\|}$ ± 1.0	124.9 ± 0.9	122.9 ** ± 0.9	121.3 $^{\#, \P}$ ± 1.2
dV/dt_{max}, V/s	272 ± 14	281 ± 11	263 ± 14	284 ± 19	282 ± 18	266 $^{\dagger, \ddagger}$ ± 19
APD_{30}, ms	2.6 ± 0.3	3.0 ± 0.4	2.7 ± 0.3	2.7 ± 0.4	3.4 ± 0.9	2.9 ± .5
APD_{50}, ms	6.1 ± 0.7	6.4 ± 0.8	5.9 $^{\#\#}$ ± 0.7	7.4 ± 1.3	7.8 ± 1.6	6.7 ± 1.2
APD_{90}, ms	25.5 ± 2.3	27.6 ± 2.7	25.5 ¶¶ ± 2.3	33.4 ± 4.1	60.3 $^{\#, \S}$ ± 9.3	44.2 ± 5.5

Values are mean ± SEM. N and n indicate number of mice and cells, respectively. Pacing rate was 1 Hz. RMP, resting membrane potential; APA, action potential amplitude; $dVdt_{max}$, maximal phase 0 upstroke velocity; APD, action potential duration; iso, isoproterenol (50 nM); WO, washout. * $P = 0.015$ vs. control; $^{\#}$ $P < 0.001$ vs. control; ** P = 0.002 vs. control; ¶ $P = 0.006$ vs. iso; § $P = 0.027$ vs. wash out; $^{\|}$ $P = 0.013$ vs. control; $^{\#\#}$ $P = 0.029$ vs. iso; ¶¶ $P = 0.048$ vs. iso; † $P = 0.003$ vs. control; ‡ $P = 0.009$ vs. iso. *P* values by *Repeated Measures ANOVA* followed by *Tukey* test for pairwise multiple comparisons.

Supplemental Table V. Properties of L-type Ca^{2+} current under conditions of high Ca^{2+} buffering

	Calm1$^{+/+}$	**Calm1$^{N98S/+}$**	***P* value**
Voltage-dependence of activation			
	n = 42, N = 5	n = 52, N = 4	
act_{half}, mV	-4.00 ± 1.2 mV	-3.1 ± 1.0 mV	0.56
k_{act}, mV	5.0 ± 0.1	5.3 ± 0.2 mV	0.60
Voltage-dependence of inactivation			
	n = 26, N = 2	n = 25, N = 2	
$inact_{half}$, mV	-9.8 ± 0.8 mV	-10.6 ± 0.8 mV	0.51
k_{inact}, mV	-5.5 ± 0.2	-5.3 ± 0.1 mV	0.53
c	0.065 ± 0.006	0.087 ± 0.006	0.013
Recovery from inactivation			
	n = 24, N = 3	n = 25, N = 3	
a	0.99 ± 0.004	0.99 ± 0.005	0.62
tau, ms	144 ± 5 ms n = 24	116 ± 6 ms n = 25	0.001

Values are mean ± SEM. N and n indicate number of mice and cells, respectively. *c*, pedestal of inactivation curve. *P* values by *t*-test (act_{half}, $inact_{half}$ and *a*) or *Mann-Whitney U* test (k_{act}, k_{inact}, and *tau)*. Parameters were calculated and averaged from individual fitting data from the number of cells indicated.

Supplemental Table VI. Properties of whole-cell $I_{Ca.L}$ under conditions of low intracellular Ca^{2+} buffering

	Calm1$^{+/+}$		**Calm1$^{N98S/+}$**	
	Control	**Isoproterenol**	**Control**	**Isoproterenol**
Voltage-dependence of activation				
	n = 11; N = 5	n = 24; N = 5	n = 11; N = 5	n = 29; N = 5
act_{half}, mV	-11.9 ± 0.9	-13.9 ± 0.8	-11.9 ± 1.4	-16.8 ± 0.8 $^{**, @}$
k_{act}, mV	6.0 ± 0.1	5.1 ± 0.5 *	6.1 ± 0.2	5.0 ± 0.1 $^{\#, ¶}$
Voltage-dependence of inactivation				
	n = 16; N = 5	n = 26; N = 4	n = 18; N = 6	n = 36; N = 4
$inact_{half}$, mV	-22.7 ± 0.8	-25.3 ± 0.7 §	-22.2 ± 0.9	-25.9 ± 0.5 $^{\#\#}$
k_{inact}, mV	-6.1 ± 0.2	-5.9 ± 0.1	-6.3 ± 0.1	-5.6 ± 0.1 $^{‖, ‡}$
c	0.098 ± 0.007	0.096 ± 0.005	0.121 ± 0.005 ¶¶	0.118 ± 0.004 †
Recovery from inactivation				
	n = 12; N = 4	n = 13; N = 3	n = 14; N = 4	n = 18; N = 3
a	1.07 ± 0.02	1.03 ± 0.01	1.06 ± 0.01	0.96 ± 0.01 $^{\&, \&\&}$
tau, ms	129.4 ± 12.0	135.4 ± 8.4	133.2 ± 7.2	124.7 ± 4.2

Values are mean ± SEM. N and n indicate number of mice and cells, respectively. * P = 0.001 vs Calm1$^{+/+}$ control by *Mann-Whitney U* test; $^{\#}$ P = 0.00001 vs. Calm1$^{N98S/+}$ control by *t*-test; ** P = 0.0035 vs. Calm1$^{N98S/+}$ control by *t*-test; ¶ P = 0.033 vs. Calm1$^{+/+}$ isoproterenol; § P = 0.028 vs. Calm1$^{+/+}$ control by *t*-test; $^{‖}$ P = 0.00008 vs. Calm1$^{N98S/+}$ control by *t*-test; $^{\#\#}$ P = 0.00028 vs. Calm1$^{N98S/+}$ control by *t*-test; ¶¶ P = 0.0117 vs. Calm1$^{+/+}$ control by *t*-test; † P = 0.00112 vs. Calm1$^{+/+}$ isoproterenol by *t*-test; ‡ P = 0.028 vs. Calm1$^{+/+}$ isoproterenol by *t*-test; $^{\&}$ P = 1*10^{e-9} vs. Calm1$^{N98S/+}$ control by *t*-test; $^{\&\&}$ P = 0.00029 vs. Calm1$^{+/+}$ isoproterenol by *t*-test; $^{@}$ P = 0.018 vs Calm1$^{+/+}$ isoproterenol by *t*-test. Parameters were calculated and averaged from individual fitting data from the number of cells indicated.

Supplemental Table VII. Properties of cardiac I_{Na}

	Calm1$^{+/+}$	**Calm1$^{N98S/+}$**
Voltage-dependence of activation		
	n = 10; N = 3	n = 7; N = 2
act_{half}, mV	-31.1 ± 1.8	-29.9 ± 1.1
k_{act}, mV	4.6 ± 0.4	5.3 ± 0.3
Voltage-dependence of inactivation		
	n = 13; N = 4	n = 14; N = 3
$inact_{half}$, mV	-59.6 ± 1.4	-60.3 ± 1.1
k_{inact}, mV	-5.6 ± 0.3	-4.6 ± 0.2
Inactivation time course (at -25 mV)		
	n = 7; N = 3	n = 7; N = 2
τ_{fast}, ms	2.5 ± 0.3	3.6 ± 0.8
τ_{slow}, ms	16.7 ± 3.7	9.9 ± 2.4
$A_{fast}/(A_{fast}+A_{slow})$	0.90 ± 0.01	0.78 ± 0.12

Values are mean ± SEM. N and n indicate number of mice and cells, respectively. act_{half}, $inact_{half}$: voltages at which (in)activation is half-maximal; k_{act}, k_{inact}: slope of (in)activation curve; τ_{fast} and τ_{slow}: fast and slow inactivation time constants; $A_{fast}/(A_{fast}+A_{slow})$: fractional amplitude of channels undergoing fast inactivation

Supplemental Table VIII. Effect of isoproterenol on *in situ* His-Purkinje myocyte action potentials.

	Calm1$^{+/+}$		**Calm1$^{N98S/+}$**	
	n = 19; N = 6		n = 19; N = 6	
	Control	**Isoproterenol**	**Control**	**Isoproterenol**
RMP, mV	-74.6 ± 1.2	-74.2 ± 1.4	-73.0 ± 1.5	-72.5 ± 1.3
APA, mV	100.2 ± 2.8	101.1 ± 3.6	93.8 ± 4.0	95.1 ± 3.7
dV/dt_{max}, V/s	145 ± 9	131 ± 10 *	129 ± 12	120 ± 11
APD_{30}, ms	13.3 ± 1.3	17.0 ± 1.6 $^{\#}$	13.2 ± 1.2	15.4 ± 1.8 **
APD_{50}, ms	22.3 ± 1.7	27.5 ± 2.2 $^{\#}$	24.8 ± 1.9	28.7 ± 2.7 **
APD_{90}, ms	70.5 ± 3.4	79.7 ± 4.6 $^{\#}$	93.3 ± 8.1 ¶	104.9 ± 6.2 $^{**, §}$

Action potentials were recorded during pacing at a cycle length of 200 ms. Values are mean ± SEM. N and n indicate number of wedges and cells, respectively. * $P = 0.018$ and $^{\#}$ $P \leq 0.002$ versus Calm1$^{+/+}$ control by *paired t-test*. ** $P < 0.02$ versus Calm1$^{N98S/+}$ control by paired *t*-test (APD_{50}) or *Wilcoxon Signed Rank* test (APD_{90}). ¶ $P = 0.041$ versus Calm1$^{+/+}$ control by *Mann Whitney Rank Sum* test. § $P = 0.002$ versus Calm1$^{+/+}$ isoproterenol by *Mann Whitney Rank Sum* test.

Supplemental Figures

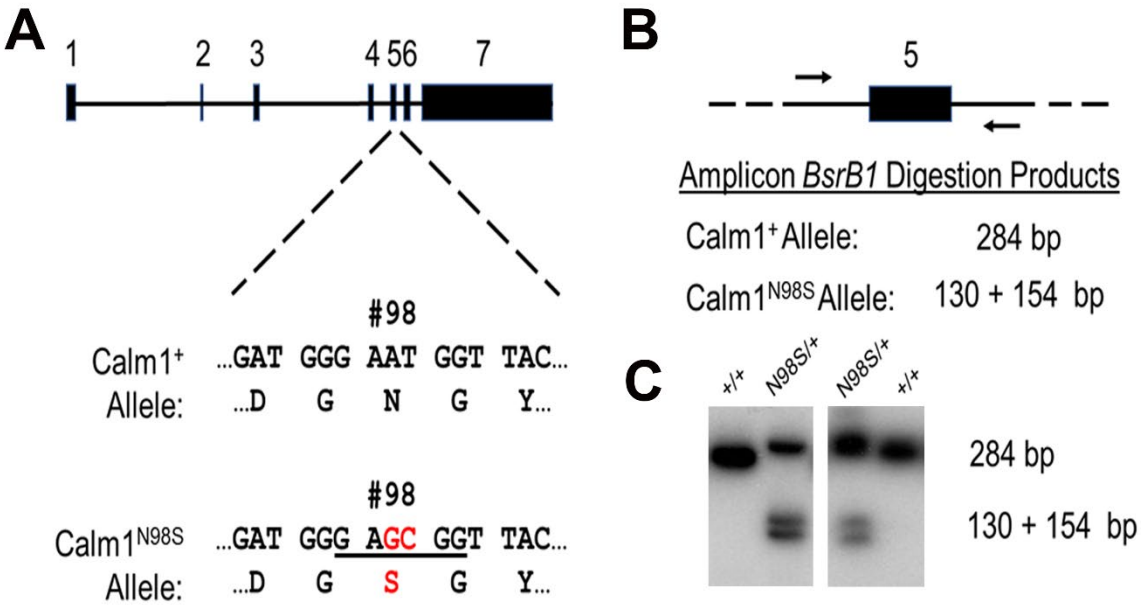

Supplemental Figure I. Generation of the N98S *Calm1* allele. **A**, Schematic of the mouse *Calm1* gene, and the sequence of the wild-type ($Calm1^{+}$) and CRISPR-generated mutant ($Calm1^{N98S}$) alleles. The CRISPR-generated nucleotide changes and the corresponding amino acid change are indicated in red. The positon of the *BsrB1* restriction site in the $Calm1^{N98S}$ allele is underlined. **B**, Schematic of the PCR amplicon spanning Calm1 exon 5, and the predicted amplicon *BsrB1* digestion products from the $Calm1^{+}$ and $Calm1^{N98S}$ alleles. **C,** PCR-based RFLP screen to monitor segregation of the $Calm1^{+}$ and $Calm1^{N98S}$ alleles. PCR amplification was performed in the presence of trace levels of α-^{32}P-dCTP, and the resulting amplicons were digested with *BsrB1*, fractionated on 8% polyacrylamide gels and visualized via autoradiography.

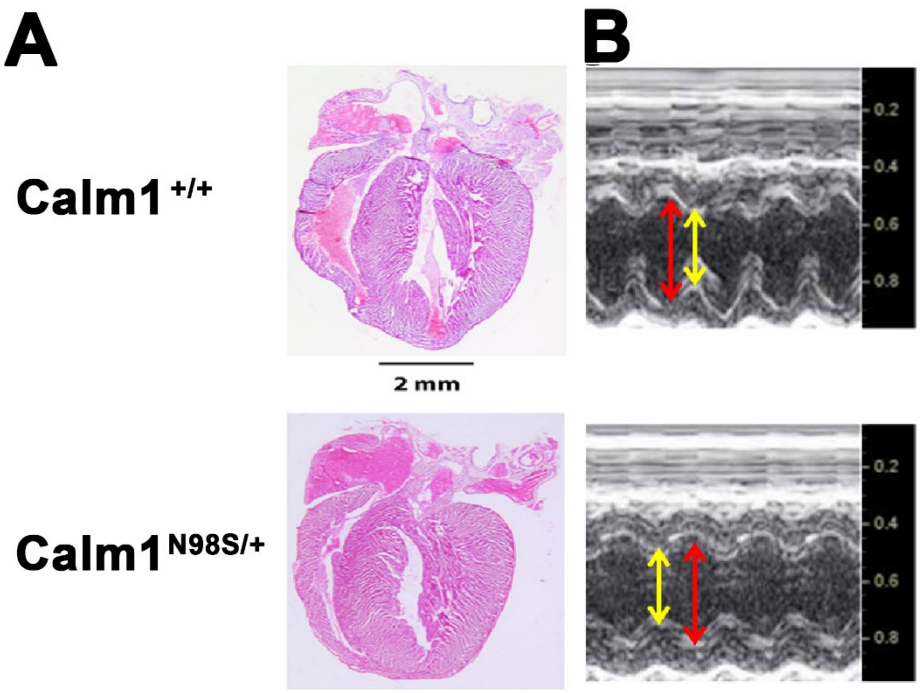

Supplemental Figure II. Calm1$^{N98S/+}$ hearts exhibit normal structure and contractile function. A, Hematoxylin & eosin-stained 4-chamber sections of a littermate Calm1$^{+/+}$ and a Calm1$^{N98S/+}$ heart at 6 months of age. **B**, M-mode echocardiograms (short-axis views) recorded in anesthetized adult Calm1$^{+/+}$ and Calm1$^{N98S/+}$ mice. Red and yellow double arrows denote left ventricular internal dimensions at end diastole and end systole, respectively.

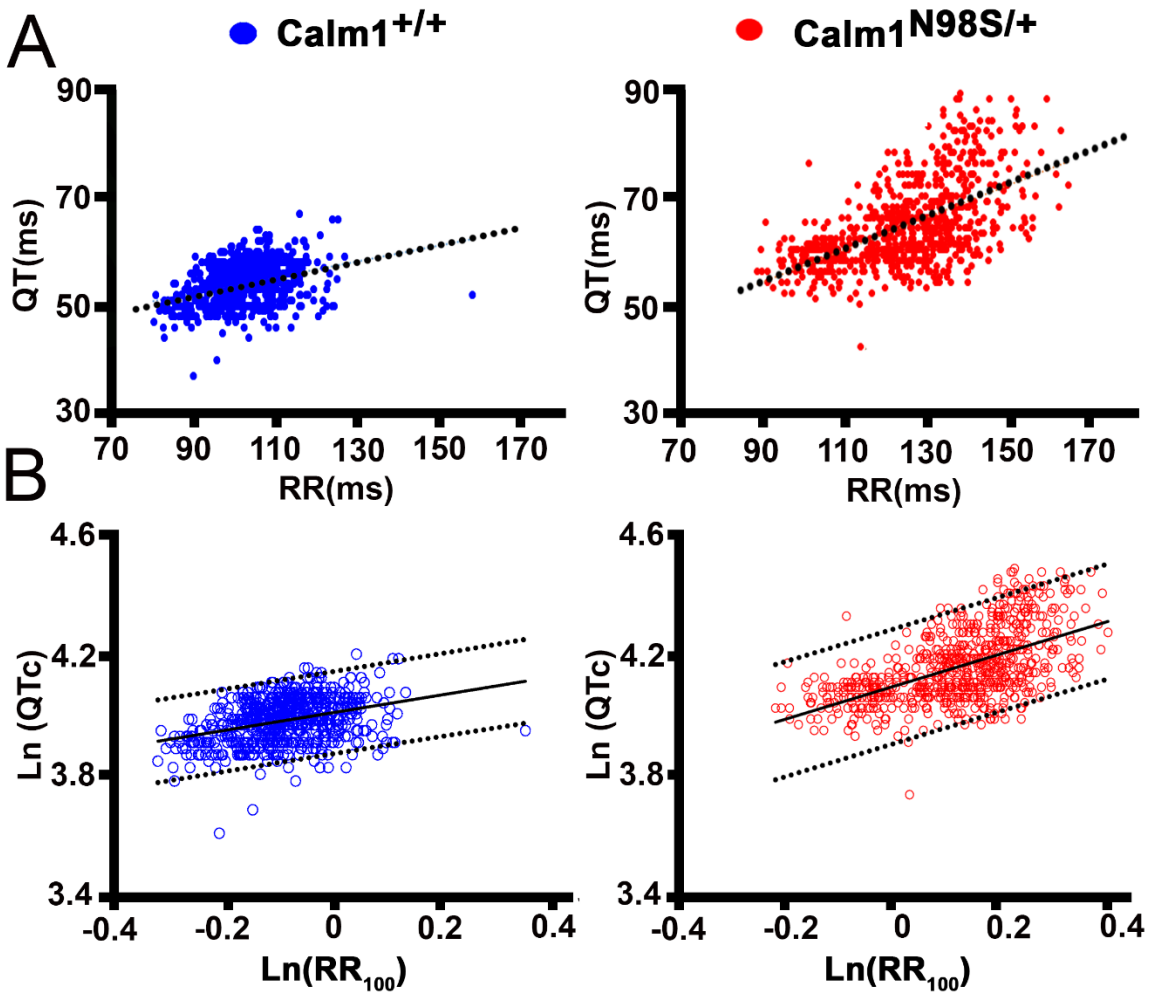

Supplemental Figure III. Analysis of QT intervals in telemetered ECGs. A, Relationships between the measured QT interval and the RR intervals in conscious male Calm1$^{+/+}$ mice (n = 9) and Calm1$^{N98S/+}$ mice (n = 10). Each point represents the average of 5- to 10-s samples taken every 20 min over a 24-hour period. Thus, there are 72 data points per individual mouse. **B**, Relationship between natural log-transformed QT intervals and normalized RR intervals in littermate control Calm1$^{+/+}$ (left) and Calm1$^{N98S/+}$ mice. Data represent all 648 and 720 measurements performed on 9 Calm1$^{+/+}$ and 10 Calm1$^{N98S/+}$ animals, respectively. QT and RR intervals were calculated from 5- to10-s samples evaluated at 20-min steps throughout the 24-h recording period. Solid and dotted lines indicate linear fits and 95% confidence intervals,

respectively. RR intervals were expressed as ratios to 110 ms. The slopes of the linear regressions were 0.29 for $Calm1^{+/+}$ mice and 0.54 for their $Calm1^{N98S/+}$ littermates ($P < 0.05$ by *Analysis of Covariance*). Identical analyses yielded a linear regression of 0.375 for both female $Calm1^{+/+}$ and $Calm1^{N98S/+}$ mice of line 2.

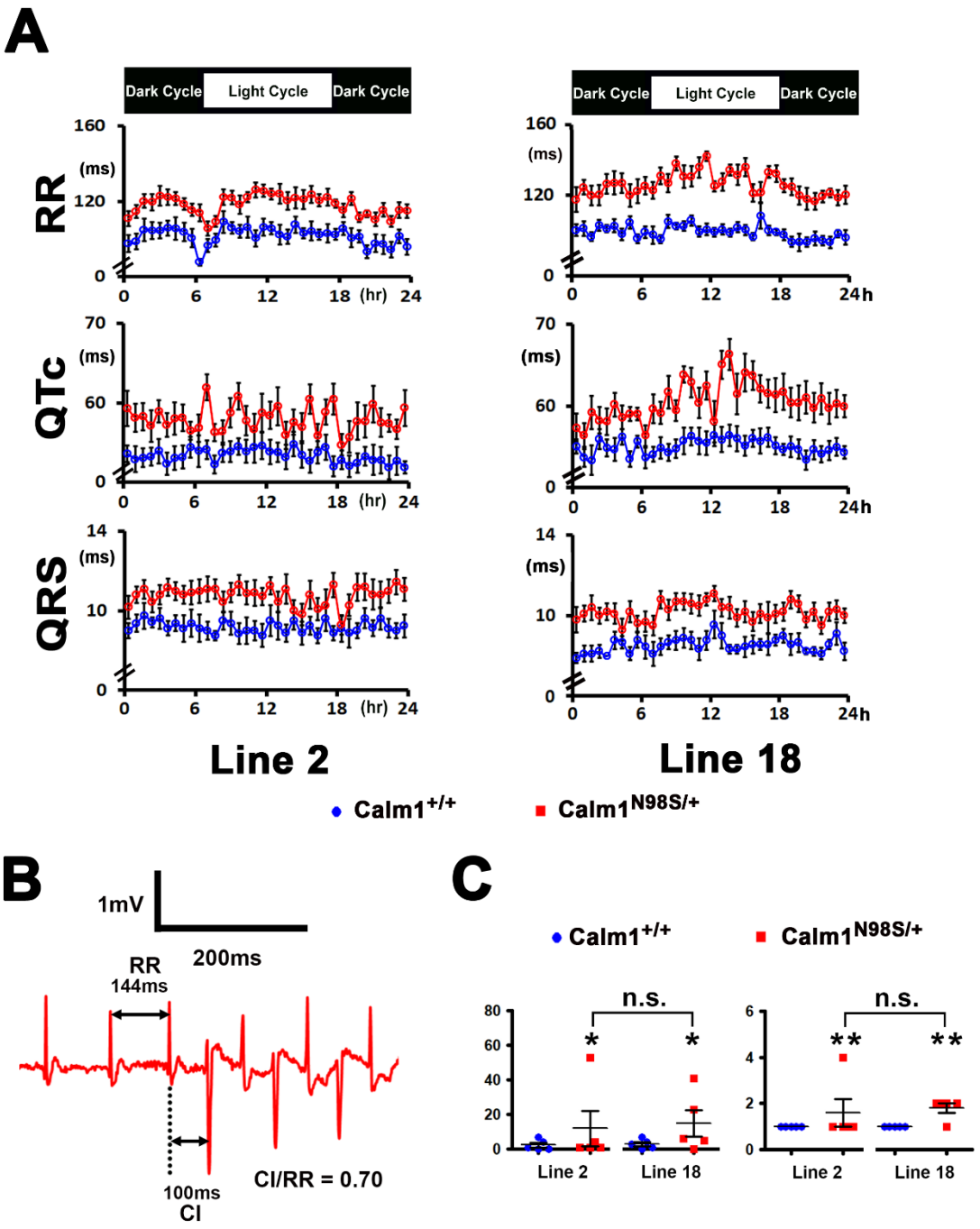

Supplemental Figure IV. Electrical phenotype in male Calm1$^{N98S/+}$ mice. A, Diurnal variations in RR interval (top), QT_c interval (middle) and QRS duration (bottom) in conscious male Calm1$^{+/+}$ and male Calm1$^{N98S/+}$ littermates of line 2 and line 18. Data are presented as mean ± SEM. Line 2: N = 8, Calm1$^{+/+}$; N = 11, Calm1$^{N98S/+}$. Line 18: N = 9, Calm1$^{+/+}$; N = 10,

Calm1$^{N98S/+}$. **B**, Coupling interval of the initiating beat of BVT in a Calm1$^{N98S/+}$ mouse. The coupling interval (CI) in ms is defined as the interval between the premature ventricular beat and the preceding sinus beat, and expressed as the ratio to the RR interval (i.e., the interval in ms between the two consecutive sinus beats preceding the tachycardia). **C,** Left panel: incidence of PVCs during 24 hours. * $P < 0.02$ versus Calm1$^{+/+}$ by *Chi-Squared* test. Right panel: 24-h arrhythmia scores. ** $P < 0.03$ versus Calm1$^{+/+}$ by *Chi-Squared* test.

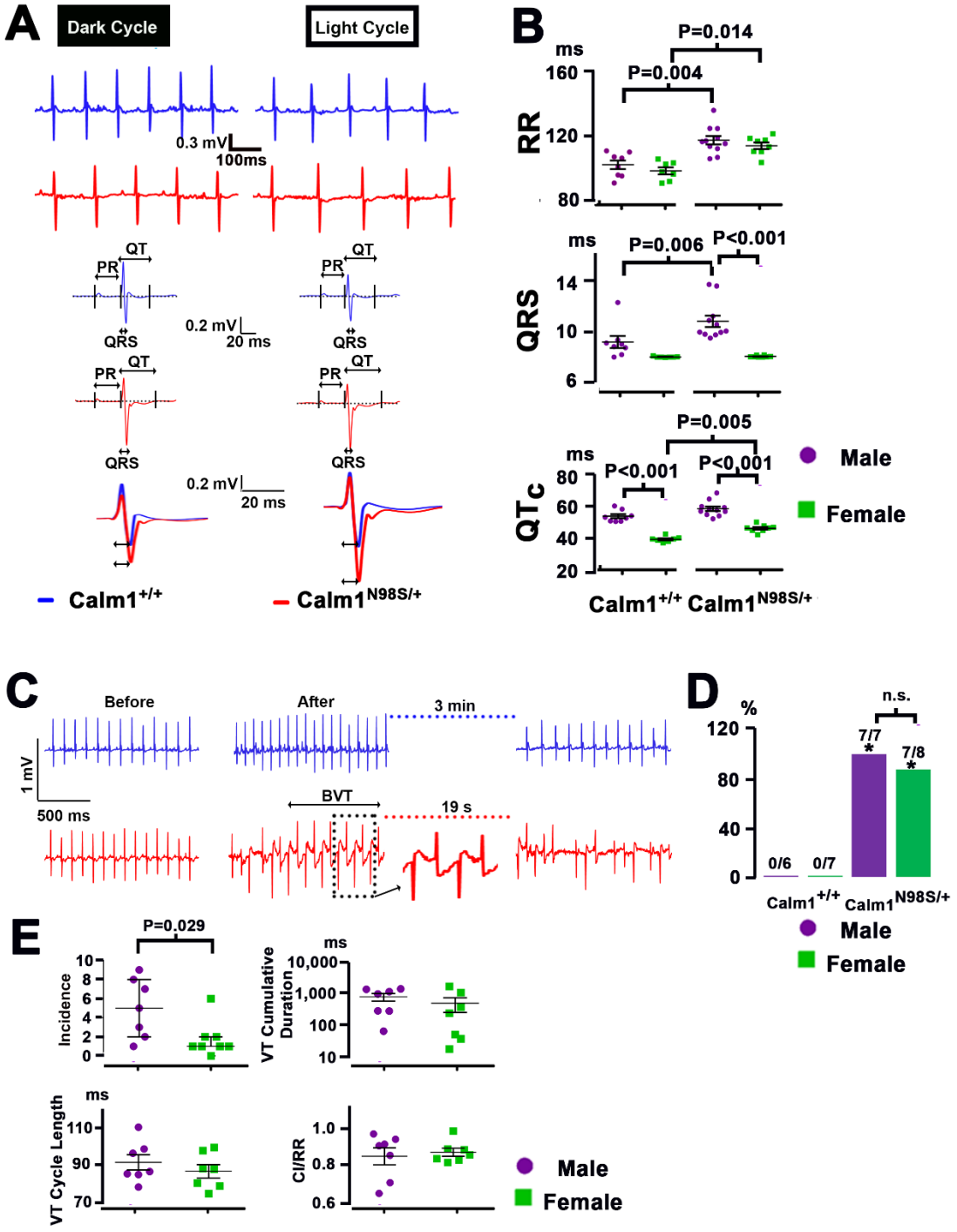

Supplemental Figure V. Electrical phenotype in female Calm1$^{N98S/+}$ mice. A, Top two rows show representative ECG traces recorded during the dark and light cycle in female Calm1$^{+/+}$ (blue) and Calm1$^{N98S/+}$ (red) littermates from line 2, revealing sinus bradycardia in the latter. Traces in the third and fourth row show signal-averaged ECGs obtained by overlaying all

consecutive cycles recorded within a 5- to 10-s interval, using QRS maximum or QRS minimum for the alignment. Bottom panels: superimpositions of signal-averaged ECGs, demonstrating absence of QRS widening in $Calm1^{N98S/+}$ mice. Arrows indicate lengths of QRS intervals. **B**, Dot plots of RR, QRS and QT_c intervals from female and male $Calm1^{+/+}$ and $Calm1^{N98S/+}$ mice of line 2. Each dot represents the 24-h average in a single animal. Horizontal lines superimposed on dots depict mean and SEM. *P* values by *One Way ANOVA* followed by *Tukey's test* for pairwise multiple comparisons. Male: 8 $Calm1^{+/+}$ and 11 $Calm1^{N98S/+}$ mice; female: 7 $Calm1^{+/+}$ and 8 $Calm1^{N98S/+}$ mice. **C**, Female $Calm1^{N98S/+}$ mice display bidirectional ventricular tachycardia (BVT). Representative telemetric ECG recordings from a conscious $Calm1^{+/+}$ and $Calm1^{N98S/+}$ female mouse obtained before and shortly after intraperitoneal injection of epinephrine (2 mg per kg body weight) and caffeine (120 mg per kg body weight). No ventricular arrhythmias were observed in the $Calm1^{+/+}$ mouse, whereas the $Calm1^{N98S/+}$ mouse developed sustained (19 s) BVT. **D**, Prevalence of BVT induced by co-administration of epinephrine and caffeine. * $P < 0.001$ versus $Calm1^{+/+}$ by *Fisher's Exact* test. **E**, Incidence, cumulative duration, cycle length and CI/RR ratio of episodes of sustained (≥ 15 s) BVT during a 30-min period of post-injection telemetric ECG recordings in conscious female and male $Calm1^{N98S/+}$ mice from line 2. Dot plots with median and interquartile range (for incidence) or mean ± SEM (for cumulative duration, cycle length and CI/RR ratio). Values are from 7 male and 7 female $Calm1^{N98S/+}$ mice. *P* value by *Mann-Whitney Rank Sum* test.

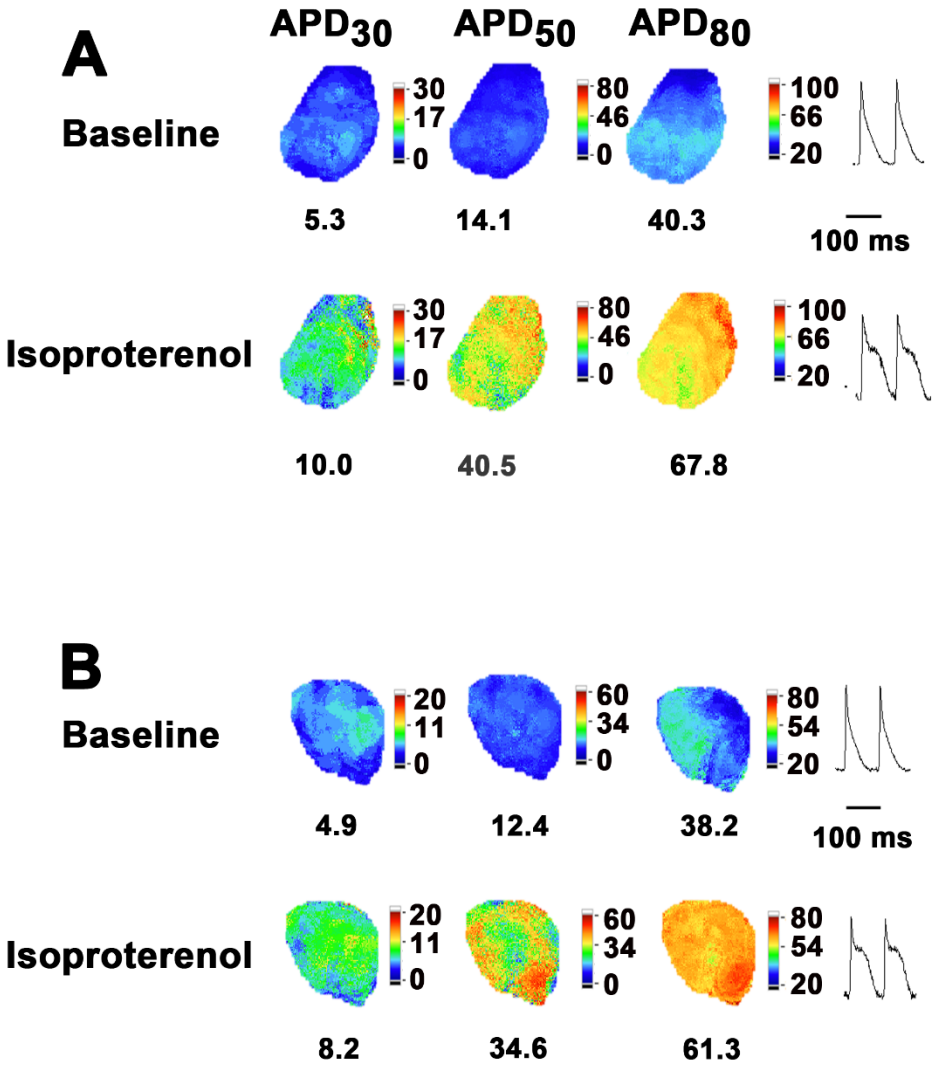

Supplemental Figure VI. β-adrenergic receptor stimulation prolongs ventricular repolarization in Calm1$^{N98S/+}$ hearts. A and **B,** Upper and lower rows in panels A and B show color-coded maps of repolarization time points at APD_{30}, APD_{50} and APD_{80} at baseline and in the presence 50 nM isoproterenol. Voltage maps were obtained during continuous atrial pacing at a cycle length of 100 ms. Traces on the right of each row represent exemplar optical action potential waveforms under control conditions and during isoproterenol exposure. Numbers below each map indicate spatially averaged values for APD_{30}, APD_{50} and APD_{80} in ms.

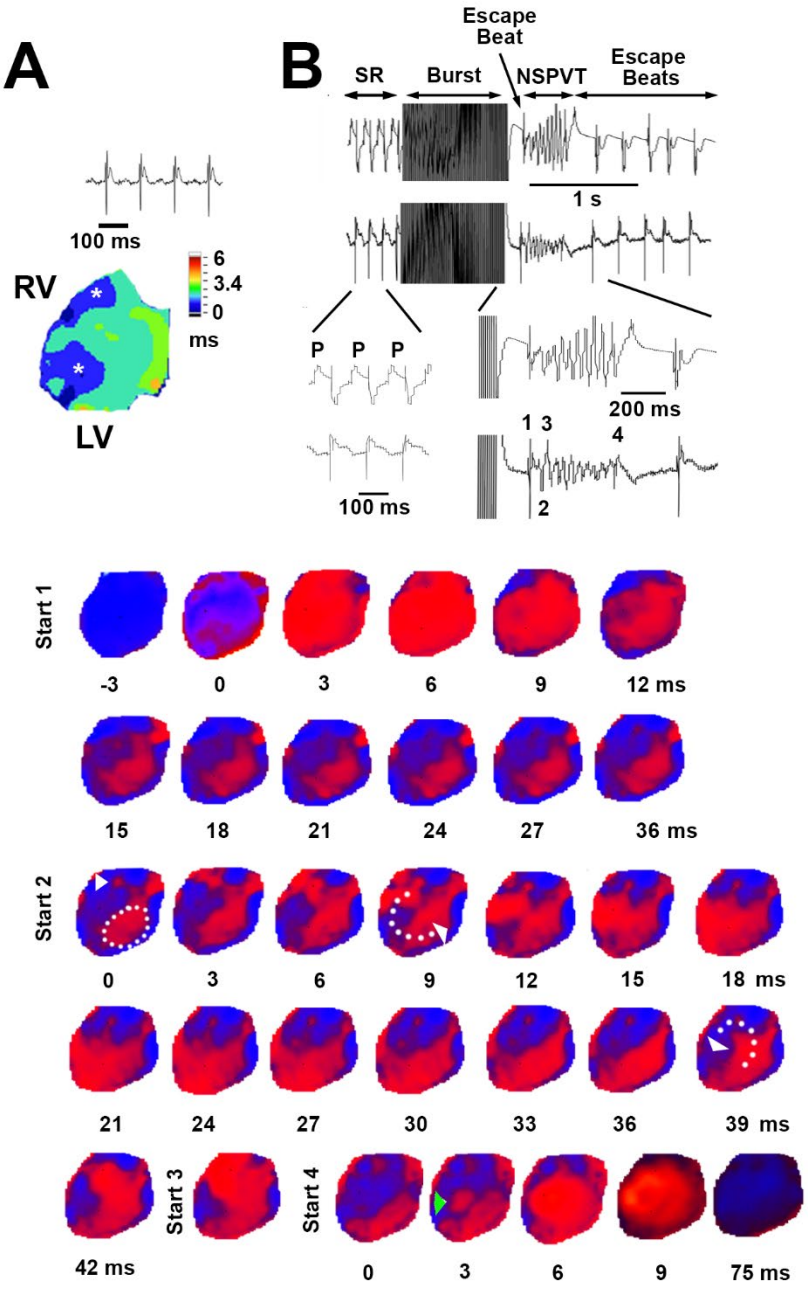

Supplemental Figure VII. Epicardial activation during ventricular tachycardia in a Calm1$^{N98S/+}$ heart. A, Volume-conducted ECG and epicardial activation map in sinus rhythm. Asterisks denote concentric breakthroughs on the anterior right and left ventricular free walls. **B,** Volume-conducted ECGs and epicardial voltage maps in the presence of 100 nM isoproterenol and 3.6 mmol/L extracellular Ca^{2+}. QRS complex numbers on ECG correspond to voltage map sequences with the same numbers. ECG shows (from left to right) sinus rhythm, a 1-s burst of

2-ms stimuli at 100 Hz, an episode of non-sustained polymorphic ventricular tachycardia (NSPVT) following an escape beat, and resumption of the escape rhythm. Map sequence 1 shows an epicardial breakthrough pattern similar to that seen during SR (panel A), suggesting a supra-Hisian origin of the first post-burst complex. The dotted circle denotes a region of long APD in the LV. The right ventricular discharge shown in map sequence 2 (arrowhead) triggers a macro-reentry revolving around the long APD region, giving rise to an R-on-T ventricular ectopic beat in the ECG. The concentric breakthrough pattern of the focal discharge was similar to that emerging from the right ventricular free wall during SR (panel A). Reentry was sustained for 8 cycles at a frequency of ~24 Hz. Termination of reentry was succeeded by the emergence of a left ventricular focal discharge (complex 4 and map sequence 4; green arrowhead). Times denote intervals after the onset of the epicardial breakthroughs.

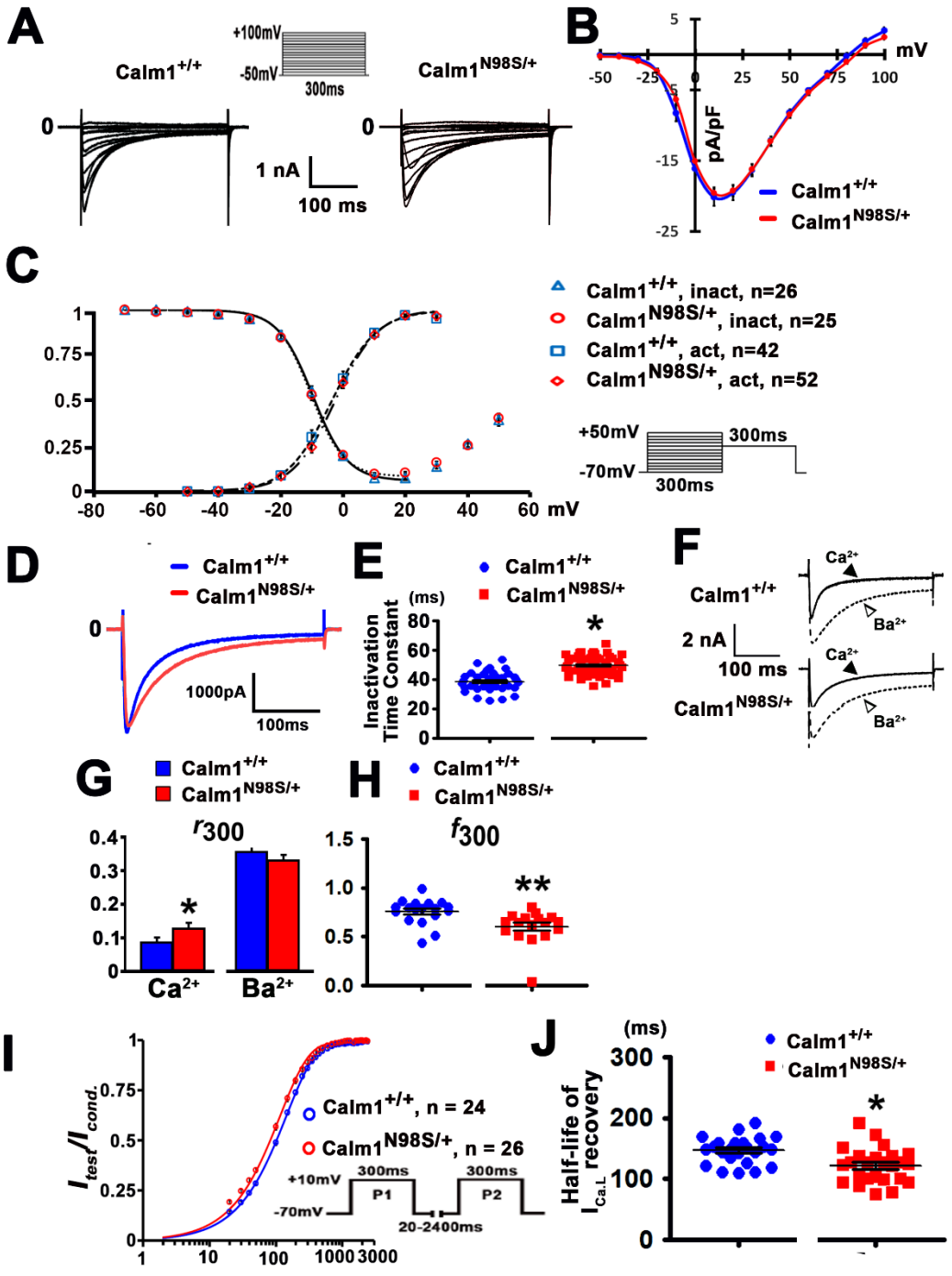

Supplemental Figure VIII. Calm1$^{N98S/+}$ ventricular myocytes exhibit diminished Ca^{2+}/CaM-dependent inactivation (CDI) of L-type Ca^{2+} channels under conditions of high intracellular Ca^{2+} buffering. A, Whole-cell $I_{Ca.L}$ evoked by 300-ms step depolarizations to voltages from -50 to +100 mV from a holding potential of -50 mV. Top: voltage-clamp protocol.

Pipette solution contained 5 μM ryanodine and 10 mM BAPTA. **B**, Pooled data for peak $I_{Ca.L}$ density as a function of test potential. Values are mean ± SEM; 42 cells from 5 $Calm1^{+/+}$ mice and 52 cells from 4 $Calm1^{N98S/+}$ mice. **C**, Voltage-dependence of steady-state $I_{Ca.L}$ activation and inactivation. Values are mean ± SEM. Solid lines are best fits of the data to a Boltzmann function (fit parameters in Supplemental Table V). There were no significant differences between the two genotypes for voltage-dependence of activation or inactivation. Activation: 42 cells from 5 $Calm1^{+/+}$ mice and 52 cells from 4 $Calm1^{N98S/+}$ mice; inactivation: 26 cells from 2 $Calm1^{+/+}$ mice and 25 cells from 2 $Calm1^{N98S/+}$ mice. **D**, Exemplar currents evoked by 300-ms step depolarization to +10 mV in a $Calm1^{+/+}$ and $Calm1^{N98S/+}$ myocyte. **E**, Dot plots of $I_{Ca.L}$ inactivation time constants. Black lines are mean and SEM. * $P = 2.7^{-13}$ by *t*-test; 42 cells from 5 $Calm1^{+/+}$ mice and 52 cells from 4 $Calm1^{N98S/+}$ mice. **F**, Representative currents evoked by +10-mV voltage step. CDI manifests as a stronger decay in Ca^{2+} current (solid line) compared to Ba^{2+} (dashed lines). **G** and **H**, Pooled data for CDI. r_{300} is the current remaining after 300 ms, normalized to peak current, whereas f_{300} equals $(r_{300,Ca} - r_{300,Ba})/r_{300,Ba}$. * $P = 0.004$ and ** $P = 0.001$ versus $Calm1^{+/+}$ by *Mann-Whitney U*-test; 18 cells from 5 $Calm1^{+/+}$ mice and 17 cells from 4 $Calm1^{N98S/+}$ mice. **I** and **J**, $I_{Ca.L}$ recovery from inactivation. **I,** Plots of $I_{test}/I_{prepulse}$ as a function of interpulse interval. Cells were held at a potential of -70 mV and were administered a 300-ms conditioning prepulse to 10 mV, followed by a variable time period at -70 mV and a 300-ms test pulse to 10 mV (see insert). Solid lines are best fits of the data to the equation $I_{test}/I_{cond} = a*[1 - \exp(-t/\tau)]$. **J**, Dot plots for $I_{Ca.L}$ recovery time constants. Horizontal lines superimposed onto the dots represent mean and SEM. * $P = 0.001$ by *Mann-Whitney U* test. Data in H and I are from 25 cells from 3 $Calm1^{+/+}$ mice and 24 cells from 3 $Calm1^{N98S/+}$ mice.

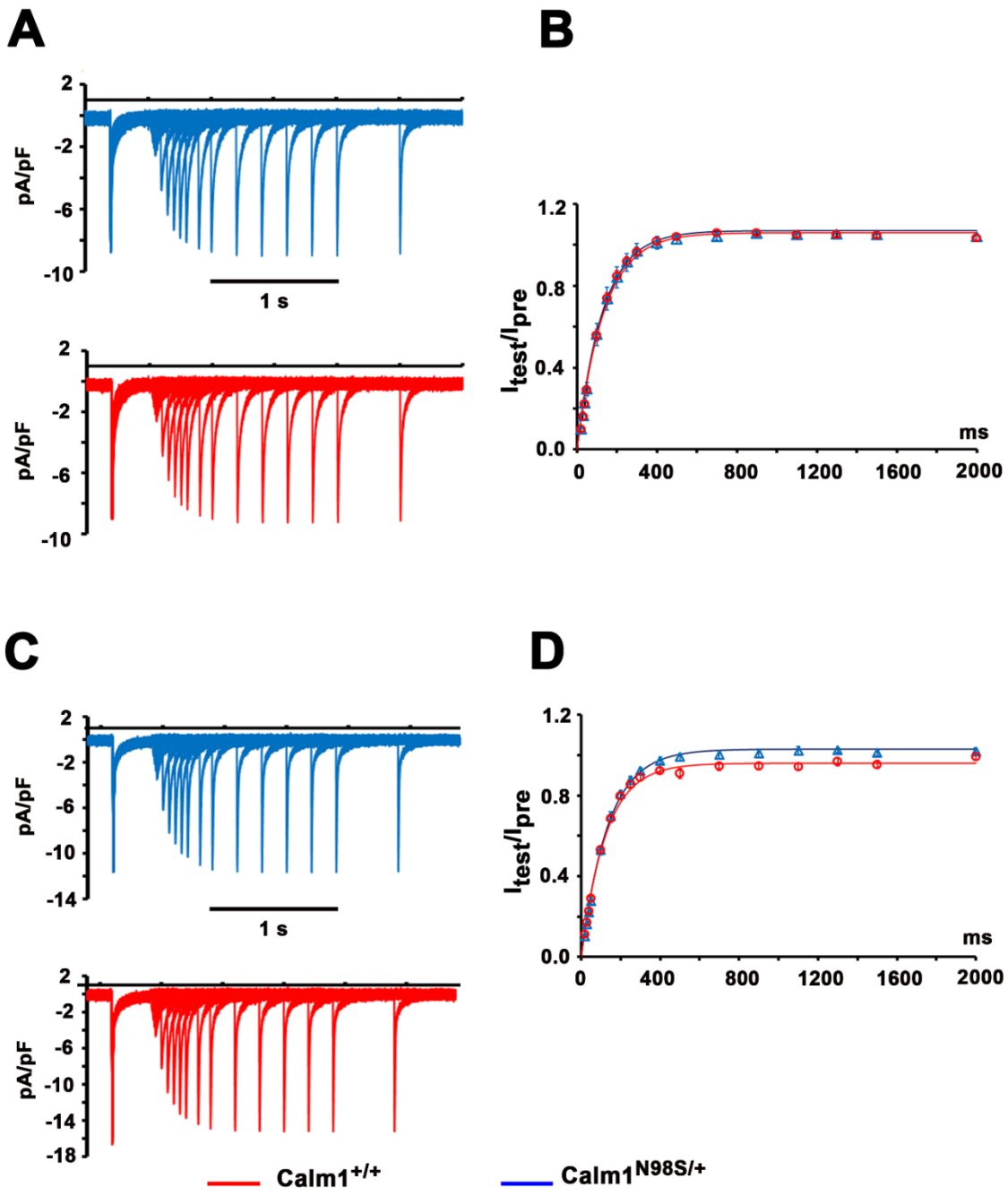

Supplemental Figure IX. $I_{Ca.L}$ recovery from inactivation under conditions of low intracellular Ca^{2+} buffering. A and **C**, Original $I_{Ca.L}$ traces for different recovery intervals in the absence (A) and presence of isoproterenol (C, 50 nM). Cells were held at a potential of -70 mV and received 300-ms conditioning prepulses to 10 mV, followed by a variable recovery period at

-70 mV and a 300-ms test pulse to 10 mV. **B** and **D**, Plots of $I_{test}/I_{prepulse}$ as a function of interpulse interval in the absence (B) and presence of isoproterenol (D, 50 nM). Values are mean ± SEM. Control: 12 cells from 4 $Calm1^{+/+}$ mice and 14 cells from 4 $Calm1^{N98S/+}$ mice. Isoproterenol: 13 cells from 3 $Calm1^{+/+}$ mice and 18 cells from 3 $Calm1^{N98S/+}$ mice. Solid lines are best fits of the data to the equation $I_{test}/I_{cond} = a*[1 - \exp(-t/\tau)]$ (fit parameters in Supplemental Table VI). $I_{Ca.L}$ recovery was incomplete in isoproterenol-treated $Calm1^{N98S/+}$ ventricular myocytes (fit parameters in Supplemental Table VI).

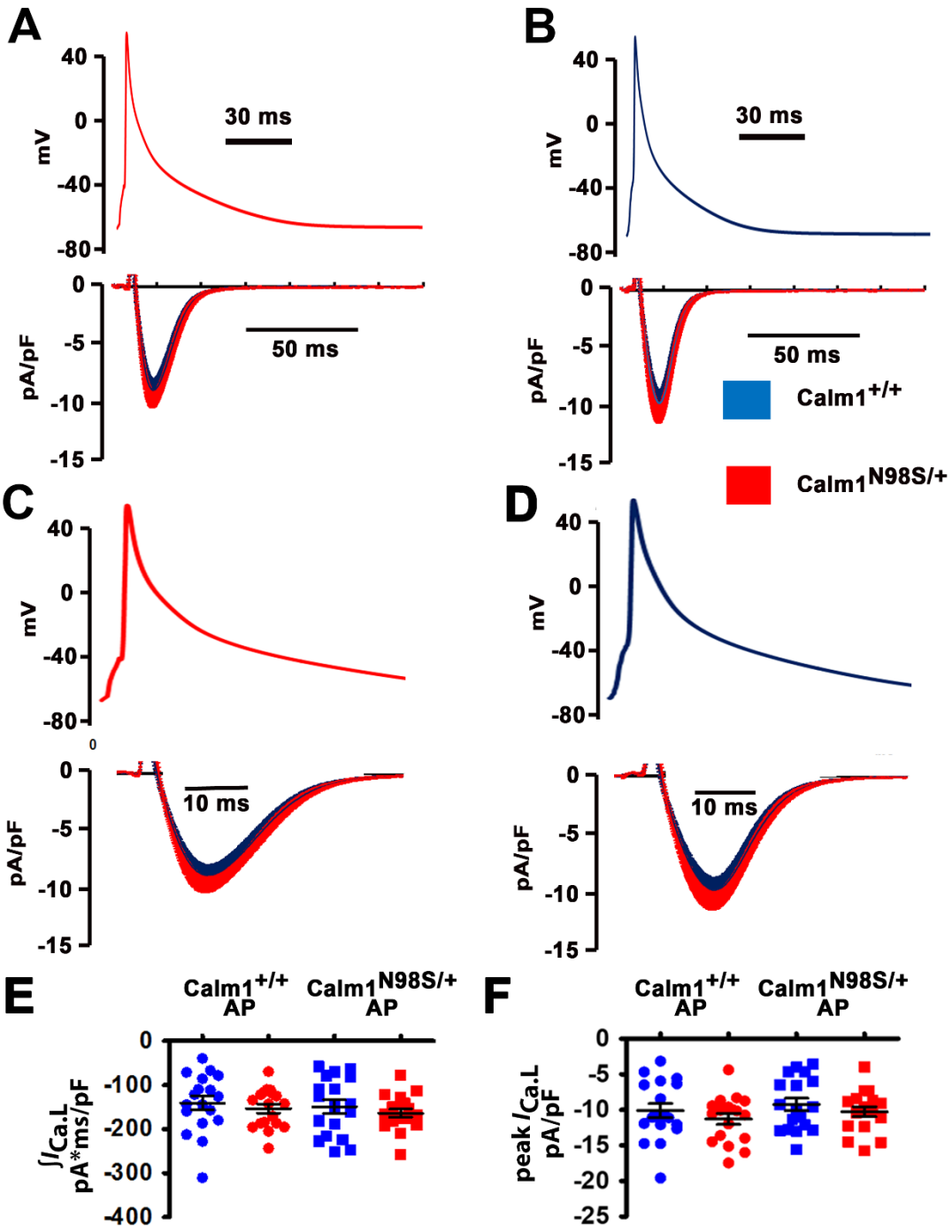

Supplemental Figure X. Whole-cell $I_{Ca.L}$ during the action potential in ventricular myocytes under control conditions. A and **B,** L-type Ca^{2+} currents (bottom panels) elicited by "typical" action potential waveforms pre-recorded from $Calm1^{+/+}$ and $Calm1^{N98S/+}$ ventricular myocytes under control conditions. Action potential waveforms were delivered at 1 Hz steady-

state frequency. Each data point in an $I_{Ca.L}$ trace represents the mean ± SEM of 18 and 18 cells distributed among 4 $Calm1^{+/+}$ and 4 $Calm1^{N98S/+}$ mice, respectively. **C** and **D**, The same action potential waveforms and action $I_{Ca.L}$ traces shown in A and B at expanded time scales. **E** and **F**, Dot plots of total $I_{Ca.L}$ normalized to cell capacitance ($\int I_{Ca.L}$; E) and peak $I_{Ca.L}$ density during the ventricular action potential. Horizontal lines indicate mean ± SEM. AP, action potential.

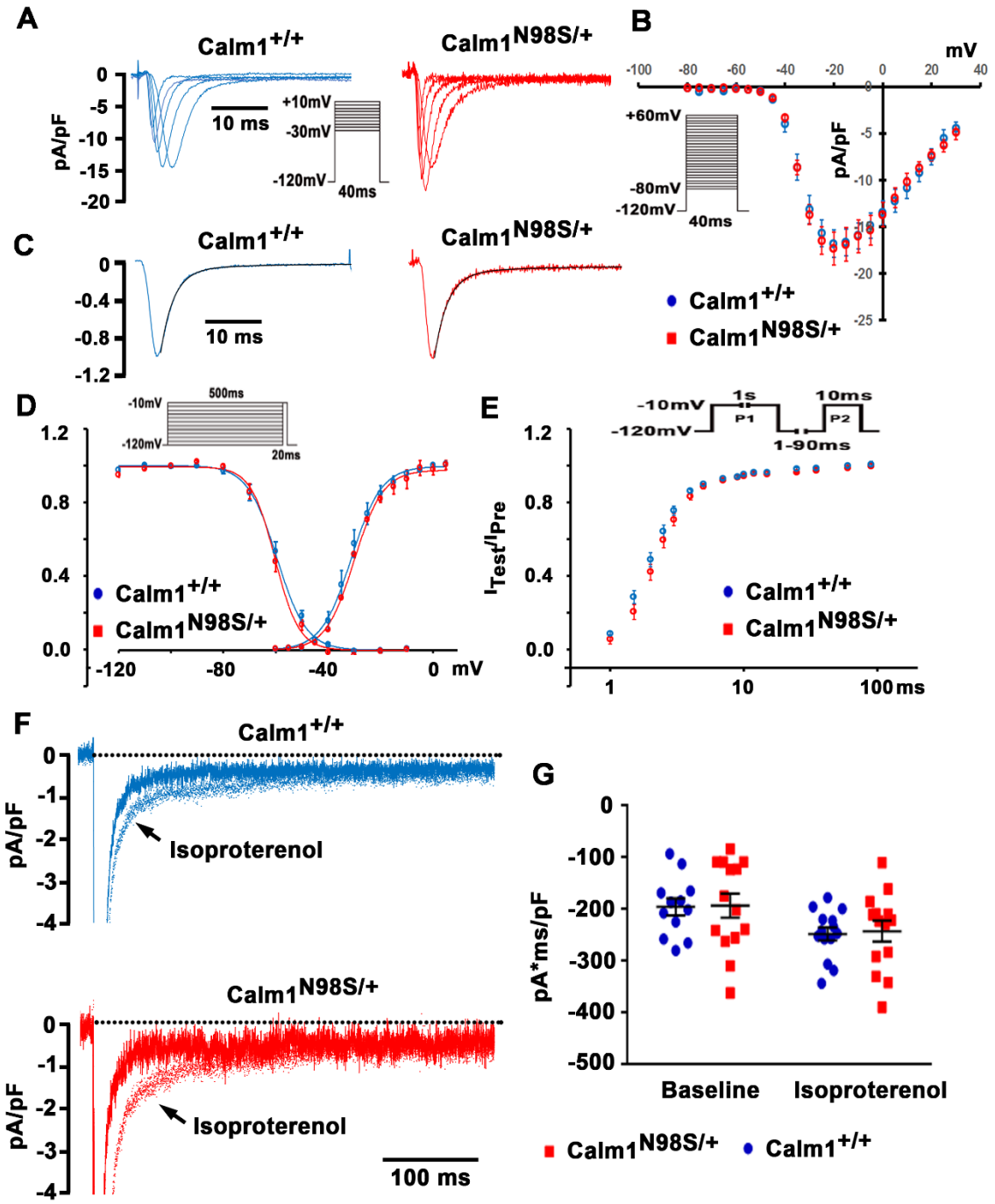

Supplemental Figure XI. Properties of cardiac voltage-gated I_{Na}. **A**, Original I_{Na} traces during 40-ms step depolarizations to potentials ranging from -30 mV to +10 mV (in 10-mV steps). **B**, Peak I_{Na} density-voltage relations. Values are mean ± SEM of 14 and 9 cells from 4 $Calm^{1+/+}$ and 2 $Calm1^{N98S/+}$ mice, respectively. The voltage-clamp protocol is shown in the inset. **C**,

Kinetics of I_{Na} inactivation. Currents were elicited at -25 mV and normalized to their respective peaks. I_{Na} decay was fit with a double exponential: $y(t) = A_{fast}\exp(-t/\tau_{fast}) + A_{slow}\exp(-t/\tau_{slow}) + y_0$. Fits are shown in black (fit parameters in Supplemental Table VII). **D**, I_{Na} steady-state activation and inactivation curves. Values are mean ± SEM (activation: 10 cells from 3 $Calm1^{+/+}$ mice and 7 cells from 2 $Calm1^{N98S/+}$ mice; inactivation: 13 cells from 4 $Calm1^{+/+}$ mice and 14 cells from 3 $Calm1^{N98S/+}$ mice). Solid lines represent averages of best-fits to Boltzmann functions for each cell (fit parameters in Supplemental Table VII). Inset: voltage-clamp protocol for steady-state inactivation. **E**, Recovery of I_{Na} from inactivation. Inset shows voltage-clamp protocol. Time intervals between paired pulses was 3 s. Values are mean ± SEM of 15 and 13 cells from 2 mice each per genotype. **F**, Original traces of I_{Na} elicited at -30 mV (for 1,000 ms) at baseline and during isoproterenol (50 nM) treatment. **G**, Dot plots of integrated I_{Na} density. Currents were integrated between 30 and 530 ms and normalized to the cell capacitance. Horizontal lines indicate the mean and the SEM (baseline: 12 cells from 3 $Calm1^{+/+}$ mice and 14 cells from 3 $Calm1^{N98S/+}$ mice; isoproterenol: 14 cells from 3 $Calm1^{+/+}$ mice and 14cells from 3 $Calm1^{N98S/+}$ mice). No significant differences were found between groups (*ANOVA*, $P > 0.05$).

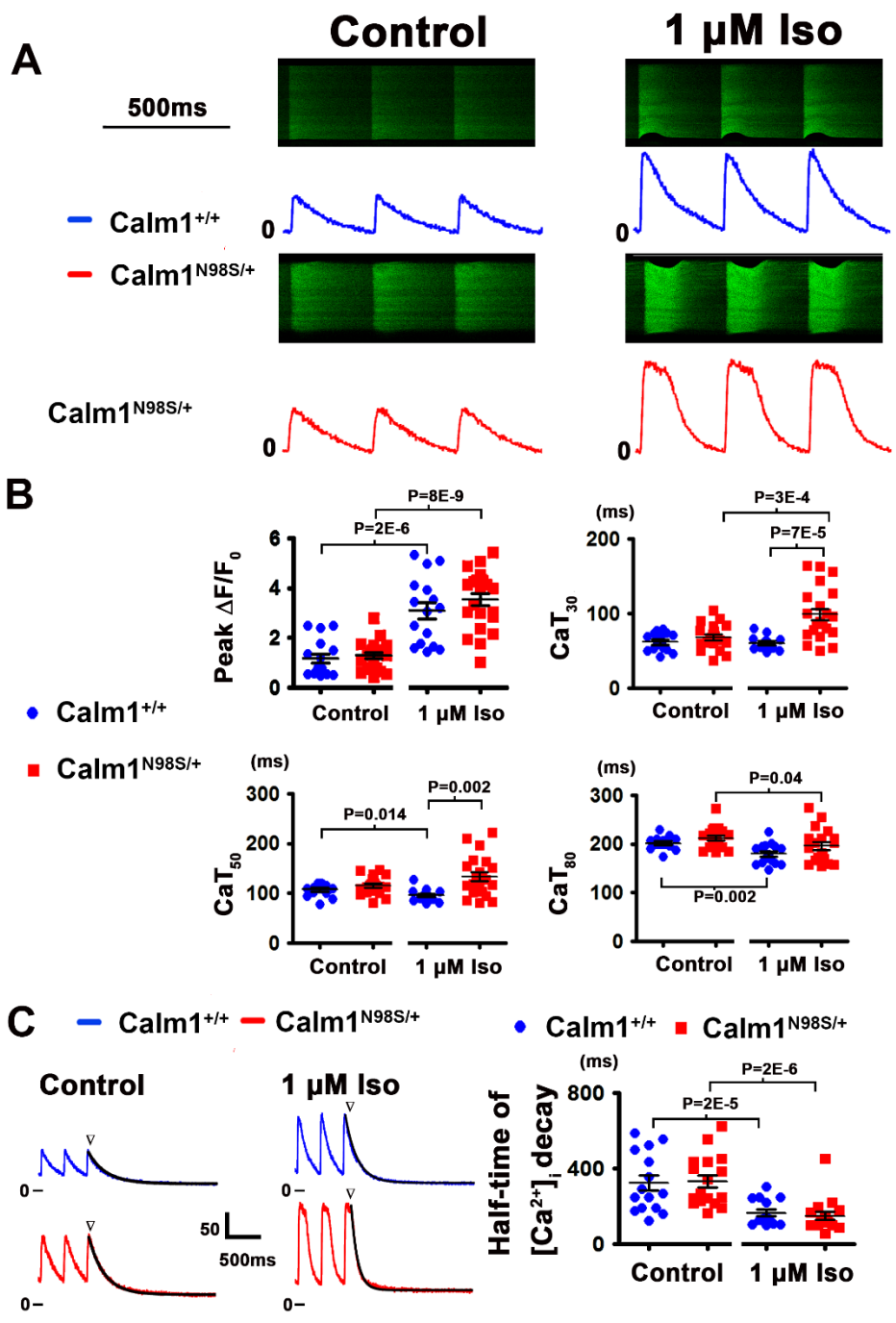

Supplemental Figure XII. N98S CaM alters response of E-C coupling to β-adrenergic receptor stimulation. A, Top, Representative confocal line-scan images of $[Ca^{2+}]_i$ transients obtained in Calm1$^{+/+}$ and Calm1$^{N98S/+}$ ventricular myocytes evoked by field stimulation at 3 Hz in the absence and presence of 1 μM isoproterenol. Bottom, Plots of line averaged $\Delta F/F_0$ as a

function of time for the corresponding line-scans shown in the top panels. **B**, Dot plots showing $[Ca^{2+}]_i$ transient amplitude and $[Ca^{2+}]_i$ transient duration at 30% (CaT_{30}), 50% (CaT_{50}) and 80% (CaT_{80}) recovery. Lines superimposed on dots represent mean and SEM. *P* values by *Wilcoxon Signed Rank* test (CaT_{50} for $Calm1^{N98S/+}$) or paired *t*-test (all others) for intragroup comparison and *Mann-Whitney U* test (CaT_{30} and CaT_{50} in the presence of isoproterenol) or unpaired *t*-test (all others) for intergroup comparisons; 17 cells from 3 $Calm1^{+/+}$ hearts and 22 cells from 3 $Calm1^{N98S/+}$ hearts. **C**, Left: Plots of line-averaged $\Delta F/F_o$ as a function of time from the same confocal line-scans in A. Black solid lines represent best fits of the $[Ca^{2+}]_i$ decay to monoexponential functions [$a = b*\exp(-t/\tau)$], starting at the times indicated by arrowheads. Right: Dot plots showing half-life of decay during 3 Hz pacing. Lines superimposed onto the dots represent mean and SEM. *P* values by paired *t*-test; 17 cells from 3 $Calm1^{+/+}$ hearts and 22 cells from 3 $Calm1^{N98S/+}$ hearts.

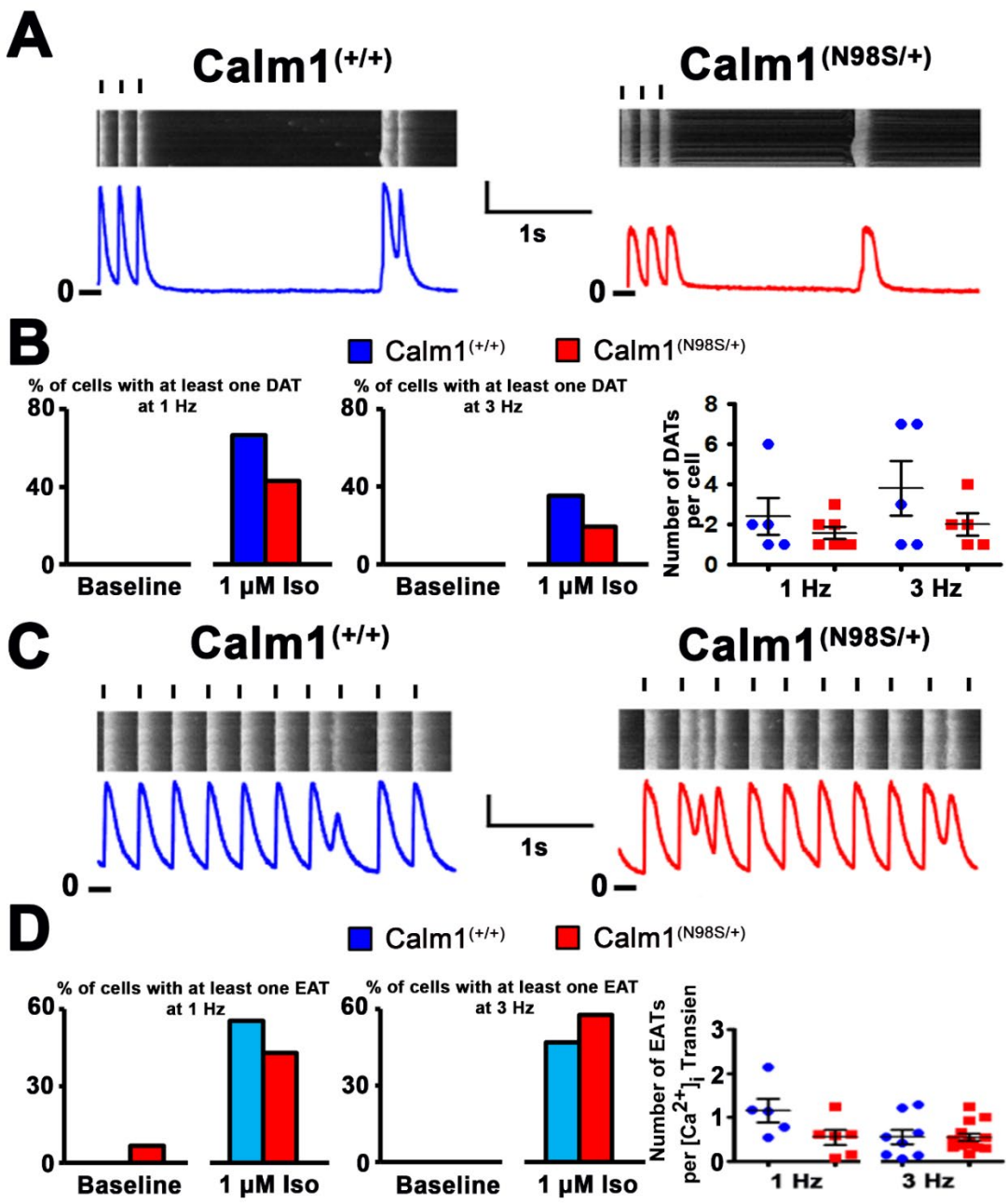

Supplemental Figure XIII. Calm1$^{N98S/+}$ myocytes lack susceptibility to Ca^{2+} aftertransients.

A, Delayed aftertransients and triggered activity observed in a Calm1$^{+/+}$ and a Calm1$^{N98S/+}$ cardiomyocyte. Line-scan images obtained from a Calm1$^{+/+}$ and Calm1$^{N98S/+}$ myocyte during and following steady state pacing at 3 Hz in the presence of 1 μM isoproterenol. The corresponding

line-averages $\Delta F/F_0$ as a function of time are shown below. After pacing stopped, the both cells show a spontaneous Ca^{2+} wave that induces two cell-wide $[Ca^{2+}]_i$ transients and one transient, respectively. **B**, Percentage of myocytes developing at least one delayed aftertransient (DAT; left and center panel) and number of repetitive DATs per cell (right panel) following steady state pacing at 1 or 3 Hz in the absence or presence of 1 μM isoproterenol. **C**, Line-scan images of early aftertransients (EATs) recorded in a $Calm1^{+/+}$ and a $Calm1^{N98S/+}$ myocyte during pacing at 3 Hz in the presence of 1 μM isoproterenol. Traces below represent line averages $\Delta F/F_0$ as a function of time. The $Calm1^{+/+}$ and $Calm1^{N98S/+}$ cell show one and two aftertransients, respectively, during the scan period. **D**, Percentage of myocytes exhibiting at least one EAT (left and center panel) and the number of repetitive EATs per $[Ca^{2+}]_i$ transient (right panel) during pacing at 1 or 3 Hz in the absence or presence of 1 μM isoproterenol.

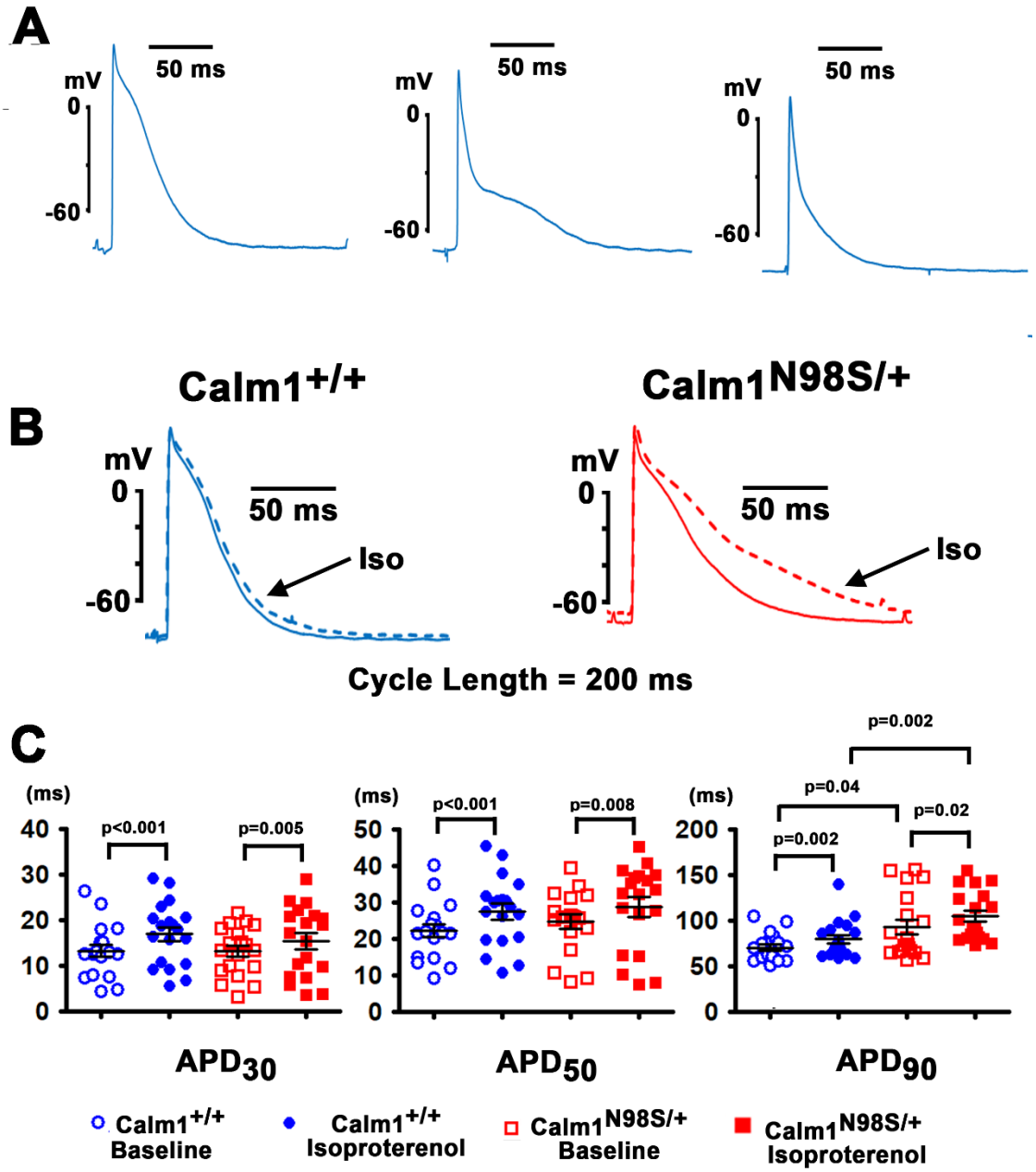

Supplemental Figure XIV. Properties of *in situ* His-Purkinje myocyte action potentials. A, Exemplary transmembrane action potentials recorded from the right bundle branch (left), the right ventricular web (middle), and the right septal endocardium (right) of Calm1$^{+/+}$ hearts. Steady-state stimulation frequency was 5 Hz. **B**, Original right bundle branch action potential recordings under control conditions and upon isoproterenol (100 nM) exposure. **C**, Dot plots of

APD_{30}, APD_{50} and APD_{90} in $Calm1^{+/+}$ and $Calm1^{N98S/+}$ His-Purkinje myocytes at control and upon isoproterenol (100 nM) stimulation. Black lines indicate mean and SEM; 19 cells from 6 $Calm1^{+/+}$ wedges and 19 cells from 6 $Calm1^{N98S/+}$ wedges. *P* values for unpaired comparisons by *t*-test (for APD_{30} and APD_{50}) or *Wilcoxon Mann-Whitney Rank Sum* test (for APD_{90}) and for paired comparisons by *Wilcoxon Signed Rank* test (for APD_{90} in $Calm1^{N98S/+}$ group) *or t*-test (all others). Additional action potential parameters are summarized in Supplemental Table VIII.